Novel haloarchaeal viruses from Lake Retba infecting *Haloferax* and *Halorubrum* species

Carolina M. Mizuno[1], Bina Prajapati[2#], Soizick Lucas-Staat[1], Telesphore Sime-Ngando[3], Patrick Forterre[1], Dennis H. Bamford[2], David Prangishvili[1], Mart Krupovic[1]*, and Hanna M. Oksanen[2]*

[1] Unité Biologie Moléculaire du Gène chez les Extrêmophiles, Institut Pasteur, 25 rue du Docteur Roux, 75015 Paris , France

[2] Molecular and Integrative Biosciences Research Programme, Faculty of Biological and Environmental Sciences, University of Helsinki, Finland

[3] CNRS UMR 6023, Université Clermont-Auvergne, Laboratoire "Microorganismes: Génome et Environnement" (LMGE), F-63000 Clermont-Ferrand, France

*Corresponding authors
Mart Krupovic
Hanna M Oksanen

[#] Current affiliation: Cell and Molecular Biology Program, Institute of Biotechnology, University of Helsinki, Finland

Running title: Haloarchaeal Viruses of Lake Retba

This article has been accepted for publication and undergone full peer review but has not been through the copyediting, typesetting, pagination and proofreading process which may lead to differences between this version and the Version of Record. Please cite this article as doi: 10.1111/1462-2920.14604

Summary

The diversity of archaeal viruses is severely undersampled compared to that of viruses infecting bacteria and eukaryotes, limiting our understanding on their evolution and environmental impacts. Here we describe the isolation and characterization of four new viruses infecting halophilic archaea from the saline Lake Retba, located close to Dakar on the coast of Senegal. Three of the viruses, HRPV10, HRPV11 and HRPV12, have enveloped pleomorphic virions and should belong to the family *Pleolipoviridae*, whereas the forth virus, HFTV1, has an icosahedral capsid and a long non-contractile tail, typical of bacterial and archaeal members of the order *Caudovirales*. Comparative genomic and phylogenomic analyses place HRPV10, HRPV11 and HRPV12 into the genus *Betapleolipovirus*, whereas HFTV1 appears to be most closely related to the unclassified *Halorubrum* virus HRTV-4. Differently from HRTV-4, HFTV1 encodes host-derived minichromosome maintenance helicase and PCNA homologs, which are likely to orchestrate its genome replication. HFTV1, the first archaeal virus isolated on a *Haloferax* strain, could also infect *Halorubrum* sp., albeit with an eight-fold lower efficiency, whereas pleolipoviruses nearly exclusively infected autochthonous *Halorubrum* strains. Mapping of the metagenomic sequences from this environment to the genomes of isolated haloarchaeal viruses showed that these known viruses are underrepresented in the available viromes.

Introduction

Hypersaline environments, where salt concentration is close to saturating, harbor a high number of virus-like particles (VLP) but rather low microbial diversity (Oren, 2002; Pagaling *et al.*, 2007; Sime-Ngando *et al.*, 2011; Ventosa *et al.*, 2015; Roux *et al.*, 2016). Although these environments are dominated by archaea and bacteria, some eukaryotes are present, e.g. the salt-adapted unicellular green alga *Dunaliella salina*, some fungi and yeast, protozoa, and the brine shrimp *Artemia* (Triantaphyllidis *et al.*, 1998; Gunde-Cimerman *et al.*, 2018). Haloarchaeal virus predation is among the most important factors driving the genetic variation of different haloarchaeal species. For instance, most of the differences between the closely related species are mapped to the genes encoding for cell surface structures and their modification, which directly affect virus-host interactions (Cuadros-Orellana *et al.*, 2007; Dyall-Smith *et al.*, 2011; Tschitschko *et al.*, 2018). As of today, more than 100 viruses have been isolated from hypersaline environments of which the majority infect extremely halophilic euryarchaea, all belonging to the class Halobacteria (Tang *et al.*, 2004; Pagaling *et al.*, 2007; Atanasova *et al.*, 2015b; Dyall-Smith *et al.*, 2019). Halophilic viruses are well adapted to high salinity and some of them remain infectious even in saturated salt (Demina *et al.*, 2016a). Some viruses can even survive in low salinities, a beneficial trait under changing environmental conditions (Pietilä *et al.*, 2013c). Halophilic archaeal viruses fall into four different morphological groups: spindle-shaped (genus *Salterprovirus*), pleomorphic (family *Pleolipoviridae*), tailless icosahedral (family *Spherolipoviridae*), and tailed icosahedral (order *Caudovirales*) (Pietilä *et al.*, 2014; Pietilä *et al.*, 2016; Demina *et al.*, 2017). However, filamentous and some exceptional morphotypes not reminiscent of any isolated virus, e.g. hairpin-shaped, bacilliform, and chain-like VLPs, have also been visualized in hypersaline water bodies (Oren *et al.*, 1997; Sime-Ngando *et al.*, 2011; Di Meglio *et al.*, 2016). Significant number of archaeal virus genes have no obvious homologs in public sequence databases (Krupovic *et al.*, 2018). Thus, classification of viral sequences in metagenomic datasets is still a challenge due to the high genetic diversity, despite of remarkable advances in next-generation sequencing and bioinformatics. In addition, the relatively low number of described halophilic archaeal virus isolates with determined complete genome sequences limits the utility of sequence similarity-based analyses. For example, only few similarities to the NCBI non-

redundant database at either the nucleotide or amino acid level were reported following the analyses of the metaviromes from hypersaline Lake Retba (Sime-Ngando *et al.*, 2011; Roux *et al.*, 2016) and halite endoliths in the Atacama Desert (Crits-Christoph *et al.*, 2016).

Two groups of haloarchaeal viruses have been frequently isolated from geographically remote locations. These include members of the family *Pleolipoviridae* and the order *Caudovirales*, respectively. Membrane-containing virions of pleolipoviruses resemble extracellular membrane vesicles able to carry the virus genome from host to host (Pietilä *et al.*, 2012). They represent a unique archaeal virus group with a recently established taxonomic position as the first family containing viruses with either single-stranded (ss) or double-stranded (ds) DNA genomes (linear or circular forms) (Pietilä *et al.*, 2016; Bamford *et al.*, 2017). The non-lytic pleomorphic virus life-cycle starts with fusion between the viral and host membranes and they exit the host cell most probably by budding, preserving the host membrane integrity (Svirskaite *et al.*, 2016; El Omari *et al.*, 2019). Their simplistic mechanism of nucleic acid transmission resembles the function of the recently described "infectious" plasmid membrane vesicles isolated from Antarctic species of haloarchaea (Erdmann *et al.*, 2017), supporting the tight evolutionary relationships between viruses and non-viral mobile genetic elements (Iranzo *et al.*, 2016b). Pleolipoviruses share a conserved core of four to five genes, mainly encoding major structural proteins of which one is the spike protein responsible for host attachment and membrane fusion (Pietilä *et al.*, 2012; Sencilo *et al.*, 2012; El Omari *et al.*, 2019).

The tailed icosahedral dsDNA viruses represent the most numerous archaeal virus group described today (Atanasova *et al.*, 2015a). Intriguingly, all these viruses infect halophiles or methanogens of the phylum Euryarchaeota (Prangishvili *et al.*, 2017). However, the identified proviruses and metagenomic studies suggest wider association of archaeal tailed viruses across different orders within the Euryarchaeota, but also with members of the phylum Thaumarchaeota (Krupovic *et al.*, 2010a; Krupovic *et al.*, 2011b; Danovaro *et al.*, 2016; Philosof *et al.*, 2017; Vik *et al.*, 2017; Abby *et al.*, 2018; Ahlgren *et al.*, 2019; Lopez-Perez *et al.*, 2019). This group of viruses shares the same architectural principles with the icosahedral tailed dsDNA bacteriophages of the order *Caudovirales* (Pietilä *et al.*, 2013b). All three different tail structures

initially characterized for bacteriophages, have been found among the archaeal viruses: long contractile (myoviruses), long non-contractile (siphoviruses), and short non-contractile tails (podoviruses) (Atanasova *et al.*, 2012). Genomes of archaeal caudoviruses are mosaics of genes with different evolutionary histories and their gene contents and genome lengths differ considerably, and consequently, also differ their capsid sizes, making this group genetically very diverse (Krupovic *et al.*, 2010a; Pietilä *et al.*, 2013c; Sencilo *et al.*, 2013; Dyall-Smith *et al.*, 2019). Although their capsid structures are very conserved, their receptor binding proteins have a high genetic plasticity allowing them to adapt to new hosts. Particularly, archaeal myoviruses with contractile tails have very broad host ranges crossing the genus boundary (Atanasova *et al.*, 2012; Atanasova *et al.*, 2015c). Furthermore, several myoviruses were shown to encode an invertible tail fiber gene module, which allows these viruses to alternate between different variants of the tail fiber proteins with distinct host specificities (Rossler *et al.*, 2004; Dyall-Smith *et al.*, 2018; Dyall-Smith *et al.*, 2019).

Both culture-independent and culture-dependent approaches indicate that haloviruses represent a globally distributed reservoir of orphan genes encoding novel functions (Aalto *et al.*, 2012; Atanasova *et al.*, 2012; Roux *et al.*, 2016). In addition, many halophilic archaea carry proviruses in their chromosomes (Krupovic *et al.*, 2010a; Dyall-Smith *et al.*, 2011; Makarova *et al.*, 2014; Liu *et al.*, 2015; Maier *et al.*, 2015; Demina *et al.*, 2016a; Atanasova *et al.*, 2018b). The co-evolution of viruses and host cells in the presence of high recombination frequency in halophilic microbes have resulted in a globally distributed complex network of viruses, proviruses, membrane vesicle, transposons, and plasmids sharing the common genetic pool and displaying dynamic interplay across time and space (Zhang *et al.*, 2012; Forterre *et al.*, 2014; Atanasova *et al.*, 2015c; Liu *et al.*, 2015; Iranzo *et al.*, 2016b; Atanasova *et al.*, 2018b; Dyall-Smith and Pfeiffer, 2018; Wang *et al.*, 2018a; Wang *et al.*, 2018b). Here we report on the isolation of four new haloarchaeal viruses from saline Lake Retba. Morphological and genomic characterization of these viruses allowed their tentative taxonomic assignments. The siphovirus HFTV1, to the best of our knowledge, is the first virus isolated on a *Haloferax* strain, and it should belong in the order *Caudovirales* with other archaeal and bacterial tailed dsDNA viruses. Bacterial and archaeal caudoviruses together with eukaryotic herpesviruses

form the HK97–like virus lineage (Abrescia *et al.*, 2012). The pleomorphic archaeal viruses might belong to a tentative new virus lineage comprising membrane vesicle-like archaeal viruses of the family *Pleolipoviridae*. Collectively, our results further expand the knowledge on the genomic diversity and host range of haloarchaeal viruses and provide insights into their genome evolution.

Results and Discussion

Isolation of novel archaeal viruses of *Halorubrum* and *Haloferax*

The viruses designated HRPV10, HRPV11, HRPV12 and HFTV1 were isolated together with their host strains from saline Lake Retba (14°50'14'' N, 17°14'55'' W), close to Dakar, the capital of Senegal, in May, 2011 (Table 1). Sample LR1 collected from the center of the Lake Retba contained grey water and a grey sediment mixed with salt, whereas sample LR2 (purple water with white sediment) was collected close to the site where salt is collected for trade. The salinity of the LR1 and LR2 samples was 290-300 g/L and 250 g/L, respectively, whereas the temperature (27°C) and pH (7.8) were the same at both sampling sites.

The haloarchaeal isolates were obtained by directly plating of the samples on MGM plates (see Methods). The obtained colonies were colony-purified on solid media. The pure cultures of the isolated halophilic archaeal strains (19 in total) were identified as members of the class *Halobacteria* by partial 16S rRNA gene sequence analysis (Fig. 1, Table 2). The isolates belong to three of the six families of the class Halobacteria: Halorubraceae (11 isolates), Haloferacaceae (7 isolates) and Halobacteriaceae (1 isolate). All isolates from Halorubraceae were identified as *Halorubrum* spp., eight of which form a clade with *Halorubrum lacusprofundi*.

LR2-19 clusters with *Hrr. sodomense*. LR1-22 clusters with an uncharacterized species of *Halorubrum* and LR2-20 did not cluster with any other strain. Among the isolates within Haloferacaceae, all seven were classified as *Haloferax* spp., clustering with *Hfx. volcanii*. LR2-15, the only representative of Halobacteriaceae, clustered with *Halomicroarcula limicola* and was classified as *Halomicroarcula* sp. LR2-15. The viruses were isolated on the endogenous Lake Retba strains (Table 2) using the same Lake Retba samples (see Methods for details). The host strains of the viruses HRPV10, HRPV11, and HRPV12 are *Halorubrum* spp. LR2-17, LR2-12, and LR1-23, respectively (Table 1), whereas HFTV1 infects *Haloferax* sp. LR2-5, making HFTV1 the first known virus isolated on *Haloferax* strain. The defective proviruses identified in *Hfx. mediterranei* (Li *et al.*, 2013) and a variant of Halorubrum virus HF1 capable of infecting *Hfx. volcanii*

[(Nuttall and Dyall-Smith, 1993) not available to our knowledge, personal communication], are the only reports on *Haloferax* viruses.

HRPV10, HRPV11, and HRPV12 produce hazy plaques that are 3-10 mm in diameter, whereas the HFTV1 plaques are clear (Table 1; Supplementary Fig. 1). The virus isolate plaque morphologies were different from each other, and HRPV10 and HRPV11, in particular, produce very hazy plaques difficult to document as figures, but they are visible in optimal lightning conditions (Supplementary Fig. 1A and B). The plaque morphologies of the HRPV10, HRPV11, and HRPV12 resemble the plaques of the members in the family *Pleolipoviridae* suggesting that also the plaques of the new pleomorphic virus isolates have non-lytic life cycle and the plaque is a consequence of the host cell growth retardation due to the virus infection (Pietilä *et al.*, 2009; Svirskaite *et al.*, 2016). The plaques were purified by three consecutive time to obtain pure virus cultures (see Methods). The virus stocks gave typical titers of 10^{11}-10^{12} pfu/ml (Table 1), suggesting that they might be promising model systems for studies on haloarchaeal virus functions and virus-host interactions. Infectivity of the viruses remained unchanged at 4 °C for a period of four weeks (data not shown).

For virus purification, virions were collected from the virus stocks by using two-step polyethylene glycol-NaCl precipitation and purified to near homogeneity by rate zonal centrifugation in sucrose followed by equilibrium centrifugation in CsCl. In the case of HRPV10, HRPV11 and HRPV12, this approach yielded highly pure virion preparations based on the specific infectivities (2-5×10^{13} pfu/mg of protein; Table 3), negative staining and transmission electron microscopy (TEM) analysis of the purified particles (Fig. 2A-C), and SDS-PAGE gel analysis (Fig. 3A-C). Specific infectivities and protein patterns of the purified HRPV10, HRPV11, and HRPV12 viruses were comparable with data reported for pleomorphic viruses purified by using the comparable precipitation and preparative ultracentrifugation techniques (e.g. viruses HRPV-1, HRPV-2, HRPV-3, HRPV-6, HHPV-1, His2, and HHPV4) yielding highly pure virus material (specific infectivities 2-5×10^{13} pfu/mg of protein) (Pietilä *et al.*, 2012; Atanasova *et al.*, 2018b). HFTV1 virus particles were purified

in high numbers based on TEM (Fig. 3D) and protein quantities (Table 3) but the purified particles had specific infectivity of ~2×10^9 pfu/mg of protein (Table 3), which is 3-4 magnitudes lower than e.g. the specific infectivities of the purified virus samples of haloarchaeal tailed virus HSTV-1 (~9×10^{12} pfu/mg of protein) and icosahedral membrane-containing virus HCIV-1 (~1×10^{12} pfu/mg of protein), of which have been analyzed structurally (Pietilä *et al.*, 2013b; Demina *et al.*, 2016b; Santos-Perez *et al.*, 2019). The negative staining and TEM of the purified HFTV1 particles revealed that some of particles had lost their genome explaining partly the loss of infectivity (Fig. 2D).

Membrane vesicle-like virions of HRPV10, HRPV11 and HRPV12

The purified HRPV10, HRPV11 and HRPV12 virions were tailless round particles with a diameter of ~55 nm (Fig. 2A-C). The virion morphologies resembled one another and those of viruses in the family *Pleolipoviridae* (Pietilä *et al.*, 2012). All three virion types equilibrated in CsCl density gradients (mean density of 1.30-1.35 g/ml) suggested that they contain lipids as one of their structural components. HRPV11 and HRPV12 were sensitive to chloroform, a widely used organic solvent, whereas HRPV10 was resistant (Table 1). Infectivity of all three viruses in the presence of non-ionic detergents Nonidet P-40 or Triton X-100 decreased by 7-11 orders of magnitude (Table 1).

The lipid compositions of the viruses and their host strains were verified by thin-layer chromatography and ammonium molybdate staining. The major polar lipids of *Haloarcula hispanica* – phosphatidylglycerol (PG), phosphatidylglycerophosphate methyl ester (PGP-Me), phosphatidylglycerosulfate (PGS), and triglycosyl glycerodiether (TGD) – have been previously identified (Bamford *et al.*, 2005) and were used as a control (Fig. 3A-C). The patterns of lipid species of *Halorubrum* sp. LR2-17, LR2-12, and LR1-23 were identical to each other, containing probably PG, PG-Me and PGS (Fig. 3A-C). In all three viruses, lipids were found to be a structural component of the virions (Fig. 3A-C). The virus lipid profiles were identical with each other and resembled the lipid profiles of their respective hosts suggesting that viruses use non-selective lipid uptake as also shown previously for other pleolipoviruses (Pietilä *et al.*, 2010; Pietilä *et al.*, 2012). Virions of all

three viruses contained two major structural protein species, which were ~60 kDa and ~7 kDa in mass when resolved in polyacrylamide gel (Fig. 3D-F). The patterns were different from each other and the major structural proteins were identified based on the gene homology to those of other pleolipoviruses (see below).

Three new pleomorphic viruses are members of the genus *Betapleolipovirus*

The nucleic acids extracted from the purified virions of HRPV10, HRPV11, and HRPV12 were sensitive to RQ1 DNase and Exonuclease III, resulting in complete degradation or extensive fragmentation, respectively. Mung bean nuclease, which is specific to ssDNA (Fig. 4A), digested the HRPV10, HRPV11, and HRPV12 genomes into discrete fragments (Fig. 4B-D), suggesting that the genomes are dsDNA molecules with nicks or single-stranded regions. Sequencing of the genomes and assembly of the reads using a *de novo* assembly algorithm (with default parameters) implemented in the CLC Genomics Workbench (QIAGEN Bioinformatics) resulted in single contigs for each genome. Each contig contained direct terminal repeats of 18-20 bp. The sequencing reads overlapping both termini were as abundant as those from other genomic positions, indicating that the genomes are circular. Consistently, assembly of the sequencing reads with the SPAdes algorithm (Bankevich *et al.*, 2012) resulted in contigs identical to those assembled with CLC Genomics Workbench, albeit with alternative start positions and terminal repeats, confirming the circular nature of the genomes (Supplementary Fig. 2).

To assess the relationship between the 3 new pleolipoviruses and the previously described members of the family *Pleolipoviridae,* we calculated intergenomic distances between pairs of viruses by pairwise comparisons of their nucleotide sequences and constructed the corresponding phylogenomic tree using VICTOR(Fig. 5A), a Genome BLAST Distance Phylogeny method (Meier-Kolthoff and Goker, 2017). The clustering of the pleolipoviruses in the resultant tree is consistent with previous classification based on the presence of genes for the putative replication-initiation or DNA polymerase proteins and relatedness of the VP3-like proteins (Pietilä *et al.*, 2016). HRPV10, HRPV11 and HRPV12 form a well-supported clade with

members of the genus *Betapleolipovirus*, namely, *Halorubrum* virus HRPV-3 and *Halogeometricum* virus HGPV-1. The clade also includes *Haloarcula* virus HHPV3 and *Natrinema* virus SNJ2, two tentative members of the *Betapleolipovirus* genus (Liu *et al.*, 2015; Bamford *et al.*, 2017).

The genomes of HRPV10, HRPV11, and HRPV12 were 9296, 9368, and 9944 bp in length, respectively, and their GC% contents were 55.2-55.7%. Genomes were predicted to contain 13-16 ORFs oriented in both transcriptional directions forming at least two putative operons (Fig. 5B; Supplementary Table 1). Genomes of HRPV10, HRPV11 and HRPV12 are very similar to each over (92-95% nucleotide identity over the whole length), but different from other characterized pleolipoviruses. The most closely related virus HGPV1 shares 68% identity over just 14% of the genome as determined by BLASTN. Consistently, comparison of the HRPV10, HRPV11 and HRPV12 proteins against the proteomes of all other known pleolipoviruses has revealed betapleolipoviruses as the closest relatives, with the largest number of sequence matches to betapleolipoviruses HGPV-1 (gene *2*, ORF5, ORF6, ORF7, ORF9, ORF13) and HRPV3 (ORF12 and ORF9), whereas ORF4 was most similar to the homolog encoded by alphapleolipovirus HHPV-2 (Supplementary Table 2). The presence of the signature gene encoding the putative replication protein (ORF11 in HRPV10) unequivocally relates HRPV10, HRPV11 and HRPV12 to betapleolipoviruses. However, single-gene phylogenies reconstructed for the core proteins, namely, spike protein (El Omari *et al.*, 2019) (Supplementary Fig. 3A) and the putative NTPase (Supplementary Fig. 3B), were not entirely consistent with this assignment (Fig. 5A), most likely reflecting occasional recombination between pleolipoviruses belonging to different genera, consistent with previous observations (Wang *et al.*, 2018a). Comparison of HRPV ORFs to the non-redundant protein sequence database reveal that the most similar sequences are found in the genomes of *Halorubrum coriense*, *Halorubrum terrestre* and *Halorubrum* sp. T3, indicating the presence of related proviruses within these organisms (Supplementary Table 1). Proviruses related to pleolipoviruses have been described in haloarchaeal strains (Liu *et al.*, 2015; Demina *et al.*, 2016a; Atanasova *et al.*, 2018a; Wang *et al.*, 2018a).

The close genetic similarity between HRPV10, HRPV11 and HRPV12 allows tracing the evolutionary events which took place in a relatively recent past. In particular, HRPV11 and HRPV12 share two small genes (HRPV11-ORF9 and HRPV12-ORF9; HRPV11-ORF14 and HRPV12-ORF15), encoding putative DNA-binding proteins carrying zinc-binding domains, which are absent in HRPV10, whereas ORF13 of HRPV12 is not found in the two other viruses (Supplementary Table 1). Notably, the closest homolog of the latter gene is encoded by an uncultivated tailed haloarchaeal virus eHP-27 (51% identity; E=3e-57) (Garcia-Heredia *et al.*, 2012), followed by homologs from diverse haloarchaea. Given that HRPV12 ORF13, which encodes a putative AdoMet-dependent methyltransferase (Supplementary Table 1), is not present in any other pleolipovirus (Fig. 5B), in all likelihood, it has been introduced into the HRPV12 genome horizontally from an unrelated haloarchaeal virus, following the divergence of HRPV12 from a common ancestor with HRPV10 and HRPV11. By contrast, the homolog of HRPV11 ORF9 has been apparently lost from the HRPV10 genome due to an inactivating point mutation, resulting in a long intergenic region between ORFs 8 and 9. Furthermore, analysis of the nucleotide similarity pattern along the HRPV10, HRPV11 and HRPV12 genomes uncovered a hypervariable region within ORF4, which encodes for a putative receptor-binding spike protein, one of the two major virion proteins suggested to be involved in host recognition and virus entry (Pietilä *et al.*, 2010). Notably, ORF4 homologs in HRPV11 and HRPV12 do not display appreciable similarity within the central region (Fig. 5B), pinpointing a highly variable protein domain, which is most likely to be critical for host recognition and binding; a similar conservation pattern is also observed in alphapleolipoviruses (e.g., compare HRPV-2 and HRPV-6 in Fig. 5B).

Comparative genomics analysis has shown that besides the five core genes conserved in all pleolipoviruses (except for His2, which contains four core genes), HRPV10, HRPV11 and HRPV12 encode several putative proteins specific to members of the genus *Betapleolipovirus*. These include homologs of HRPV10 ORF8 and ORF11, which are conserved in all currently known betapleolipoviruses, as well as ORF10 and ORF13, conserved in a subset of betapleolipoviruses, but not in viruses from the two other genera (Fig. 5B). Previous sequence analyses did not provide insights into the putative functions of the four conserved proteins. Indeed, HRPV10 ORF11-like proteins, which were suggested to represent replication initiation

proteins of betapleolipoviruses (Krupovic *et al.*, 2018), remain recalcitrant to functional annotation based on sequence similarity searches. However, profile-profile comparisons initiated with the sequence of HRPV10 ORF8 revealed homology to various PD-(D/E)XK family nuclease, including type II restriction endonucleases (Supplementary Table 1). Notably, the protein is not restricted to betapleolipoviruses, but is also conserved in several other groups of unrelated haloarchaeal viruses, including members of the *Caudovirales* (HHTV-1) and *Sphaerolipoviridae* (SH1, PH1, HCIV-1, HHIV-2). HRPV10 ORF10 and ORF13 encode putative DNA-binding proteins with winged helix-turn-helix and ribbon-helix-helix domains, respectively (Supplementary Table 1), and may be involved in transcriptional regulation of the viral and/or host genes.

The first virus isolated on *Haloferax* has an icosahedral head, non-contractile tail and circularly permuted dsDNA genome

Micrographs of the purified HFTV1 virions revealed icosahedral particles with a long non-contractile tail typical of the siphovirus morphotype (Fig. 2D). The diameter of the head was ~50 nm and the tail length was ~60 nm. The major protein species of HFTV1 virions were approximately 50, 40, 22 and 16 kDa in mass (Fig. 3G). The infectivity of HFTV1 in the presence of chloroform, Nonidet P-40, or Triton X-100 remained unchanged (Table 1), suggesting that the virion does not contain a membrane moiety and consists only of proteins and nucleic acid.

The nucleic acid extracted from purified HFTV1 virions was sensitive to RQ1 DNase treatment, but resistant to Exonuclease III and Mung bean nuclease, indicating that the genome is a dsDNA molecule (Supplementary Fig. 4). Genome sequencing and read assembly were performed as described above for pleolipoviruses and yielded a 38,059 bp-long circular contig (GC% ~54%), which appears to represent a complete viral genome. A total of 70 ORFs were predicted in the HFTV1 genome using Prodigal (Hyatt *et al.*, 2010), of which 28 (40%) did not have any clear homologs in the public databases (Supplementary Table 3, Supplementary Fig. 5). Half (35) of the gene products had sequence similarity (35-84% identity;

Supplementary Table 3) to haloviruses: 15 to halophilic archaeal siphovirus HRTV-4 originating from a salt water sample from Margherita di Savoia, Italy (Sencilo *et al.*, 2013), and 20 to uncultivated environmental haloviruses identified in the solar saltern of Santa Pola, Spain (Garcia-Heredia *et al.*, 2012). The remaining 10% of the genes had closest homologs encoded in cellular organisms. Namely, the most significant similarities were shared with archaea from the order Halobacteriales (*Natrialba, Natronobacterium, Haloarcula, Halococcus* and *Haloterrigena*) and one to *Cellulophaga baltica*, a marine bacterium from the order Flavobacteriales (Supplementary Fig. 5). All ORFs but one are arranged in the same transcriptional direction (Fig. 6).

To determine the packaging mechanism employed by HFTV1, we analyzed the bias in distribution of the 1,657,094 sequencing reads along the HFTV1 genome using PhageTerm, a tool that relies on the detection of biases in the number of sequencing reads observable at natural DNA termini compared with the rest of the viral genome (Garneau *et al.*, 2017). The analysis revealed a pattern of sequencing read coverage consistent with a circularly permuted, terminally redundant genome and headful packaging mechanism initiated from a *pac* site, similar to that of bacteriophage P1 (Supplementary Fig. 6). Consistently, phylogeny of the large subunit of the terminase (Supplementary Fig. 3B), an enzyme responsible for genome packaging in bacterial and archaeal members of the order *Caudovirales*, revealed a relatively close relationship of HFTV1 to *Halorubrum* virus HRTV-4, a siphovirus for which the genome was also found to be circularly permuted (Sencilo *et al.*, 2013).

The phylogenomic analysis using VICTOR (Meier-Kolthoff and Goker, 2017) confirmed the relationship of HFTV1 with *Halorubrum* virus HRTV-4, and also revealed relationship to four uncultivated viruses, eHP-1, eHP-15, eHP-19 and eHP-34 (Garcia-Heredia *et al.*, 2012), for which the hosts have not been previously predicted (Supplementary Fig. 7A). The genomes of the latter viruses are generally collinear with those of HFTV1 and HRTV-4. The highest sequence similarity between the genomes is observed within the genes encoding for putative virion morphogenesis proteins, such as the major capsid protein, the large subunit of

the terminase and tail proteins (Fig. 6). Given this genomic conservation, we predict that the uncultivated HFTV1-like viruses eHP-1, eHP-15, eHP-19 and eHP-34 infect halophilic archaea.

The genome of HFTV1 encodes several proteins putatively involved in DNA metabolism, namely a replicative minichromosome maintenance (MCM) helicase (gp58), DNA polymerase sliding clamp protein PCNA (gp64), DNA methyltransferase (gp61) and Rad52-like recombinase (gp50) (Fig. 6, Supplementary Table 3). The MCM is the principal helicase responsible for unwinding of the dsDNA duplex during chromosomal replication in archaea and eukaryotes (Bell and Botchan, 2013). MCM homologs have been previously identified in archaeal viruses and plasmids with moderately-sized genomes (20-50 kb) (Krupovic *et al.*, 2018) and phylogenetic analyses have suggested that mobile genetic elements have horizontally acquired the *mcm* genes from cellular organisms on multiple independent occasions (Krupovic *et al.*, 2010b). The PCNA sliding clamp is another key replication protein in archaea and eukaryotes and is known as a "molecular tool-belt" due to its interaction with multiple other proteins involved in DNA replication and repair, including replicative DNA polymerase, DNA ligase, replication factor C, Flap Endonuclease 1 (FEN1) and RNase H (Pan *et al.*, 2011). Similar to MCM helicases, PCNA homologs have been previously identified in some haloarchaeal virus genomes (Raymann *et al.*, 2014), whereas certain other archaeal viruses have been shown to specifically recruit the host PCNA for the replication of their genomes (Gardner *et al.*, 2014). Thus, the virus-encoded MCM and PCNA homologs are likely to orchestrate the replication of the HFTV1 genome.

Despite the synteny within the morphogenetic gene modules of HFTV1, HRTV-4, eHP-1, eHP-15, eHP-19, and eHP-34, the genome replication modules of these viruses appear to be very different. Namely, among the five viruses, only HFTV1 encodes both MCM helicase and PCNA. Notably, there is only one other known archaeal halophilic virus, podovirus HSTV-1, which harbors genes for both proteins in its genome (Pietilä *et al.*, 2013b; Raymann *et al.*, 2014). By contrast, the MCM helicase is encoded only by eHP-34, whereas HRTV-4, the closest relative of HFTV1, as well as eHP-1, eHP-15 and eHP-19 do not encode either of the two replication proteins. These observations reaffirm that virion formation and genome replication are

uncoupled processes and evolve independently (Krupovic and Bamford, 2010), as is also evident in the case of pleolipoviruses, where viruses from the three genera encode non-homologous genome replication proteins (Krupovic *et al.*, 2018). Consequently, viral genomes are often mosaics of genes with different evolutionary histories (Juhala *et al.*, 2000; Pope *et al.*, 2015; Iranzo *et al.*, 2016a; Yutin *et al.*, 2018).

Genetic mosaicism in tailed bacteriophage genomes is thought to be generated by illegitimate recombination (Krupovic *et al.*, 2011a) or relaxed homologous recombination (De Paepe *et al.*, 2014). The former occurs at essentially random positions within the genome, with nonviable recombinants being purged by natural selection (Pedulla *et al.*, 2003). The latter process involves promiscuous phage-encoded recombinases, such as phage λ recombinase Redβ, which catalyze homologous recombination by annealing short and diverged sequences (De Paepe *et al.*, 2014). Among the phage recombinases, the Rad52-like family is by far the largest and most diversified (Lopes *et al.*, 2010). Interestingly, HFTV1 encodes a divergent member (gp50) of the Rad52-like family of recombinases (Rad52, PDB profile 5JRB_A, HHpred probability of 94%), which might facilitate genome remodeling in the replication modules of HFTV1-like viruses. Homologs of HFTV1 gp50 are also encoded by HRTV-4, eHP-1, eHP-15, and eHP-34 as well as by several other uncultivated halophilic viruses. Notably, the closest homologs of the HFTV1 PCNA are encoded by cellular organisms, suggesting that the corresponding gene has been acquired by HFTV1 from halophilic archaea, rather than inherited from a common ancestor shared with other viruses. Similarly, the closest homologs of the orthologous HFTV1 and eHP-34 MCM helicases are encoded by halophilic archaea, whereas homologs from other viral groups are more divergent. This suggests that the *pcna* and *mcm* genes have been acquired directly from the hosts in different groups of archaeal viruses on several occasions, independently of each other.

Narrow host range of haloarchaeal viruses from Lake Retba

To determine the host range of viruses isolated from Lake Retba, we first tested their infectivity towards the 19 autochthonous haloarchaeal strains (Table 2). Despite the overall close genomic similarity, the

pleomorphic viruses HRPV10, HRPV11, and HRPV12 were found to have distinct host ranges. HRPV11 displayed the broadest host range, being able to infect four different *Halorubrum* strains isolated from Lake Retba, whereas HRPV10 and HRPV12 each could infect only two different strains. *Halorubrum* sp. LR2-12 was susceptible to all three pleomorphic viruses, albeit with highly different efficiencies of plating (EOP) (Table 2). Notably, *Haloferax* virus HFTV1 was found to infect hosts across the genus boundary. In addition to its own isolation host, LR2-5, belonging to the genus *Haloferax* (Table 2), HFTV1 was able to infect *Halorubrum* sp. LR1-23, albeit with an eight orders of magnitude lower efficiency (Table 2). Similarly, a previous cross-infectivity study has shown that haloarchaeal siphoviruses generally display genus-restricted host ranges, although some isolates were found to infect hosts belonging to two or three genera (Atanasova *et al.*, 2015c).

Next, we set out to explore the infectivity of the four viruses against *Haloferax* and *Halorubrum* strains isolated from geographically remote locations (Israel, Italy, Slovenia, Spain, Thailand and Antarctica). Namely, we tested 41 distinct *Halorubrum* strains originating from 10 different sampling sites and seven *Haloferax* strains from five distinct locations (Supplementary Table 4). Among the 51 strains tested, only *Halorubrum* sp. E200-4 isolated from Eilat, Israel was sensitive to pleomorphic virus HRPV11, albeit with a considerably lower (~6×10^{-3}) EOP. This observation is consistent with the previous finding that most pleolipoviruses are highly specific to their isolation hosts (Atanasova *et al.*, 2012; Atanasova *et al.*, 2015c), but also indicates that occasional cross-infections that transcend site and time of isolation are possible. Similar patterns of infection, whereby viruses preferentially infect hosts from the same site rather than hosts isolated from similar but geographically remote sites, are also typical of bacterial virus-host systems from different ecological niches (Vos *et al.*, 2009; Koskella *et al.*, 2011), including hypersaline environments (Villamor *et al.*, 2018). Thus, a pronounced biogeographical pattern emerges in haloarchaeal virus-host interactions, possibly due to increased diversification of the species composition of communities as a function of increasing geographic and environmental distance (Weitz *et al.*, 2013). The specificity of viruses to autochthonous strains seemingly contrasts the conclusions drawn from comparative (meta)genomic analysis of halophilic viral communities which indicated that hypersaline viral communities should be

considered as a genetic continuum across continents (Roux *et al.*, 2016). Collectively, the results of the large-scale comparative genomics and local infectivity studies suggest that the gene complements responsible for virion formation and adaptation to environmental conditions are shared by haloarchaeal viruses across the globe, whereas the incessant evolutionary arms race drives local adaptation of viruses and their hosts at a finer scale.

Haloarchaeal myovirus isolates appear to display a broader host range (Atanasova *et al.*, 2012; Atanasova *et al.*, 2015c) than siphoviruses, such as HFTV1. This tendency appears to be general, because bacterial myoviruses also display broader host range than siphoviruses and podoviruses (Wichels *et al.*, 1998). The broader host range of archaeal myoviruses might be linked to the larger genomes and, accordingly, functionally more diverse gene content (Krupovic *et al.*, 2018) including e.g. many auxiliary genes involved in DNA and RNA metabolism (Sencilo *et al.*, 2013). For instance, HVTV-1 encodes an almost complete replisome (Pietilä *et al.*, 2013c; Kazlauskas *et al.*, 2016), whereas HGTV-1 encodes an RNA ligase and lysyl-tRNA synthetase and has 36 tRNA genes for all universal genetic code amino acids (Sencilo *et al.*, 2013). Presumably, this extended gene baggage renders myoviruses more promiscuous and partly independent of the corresponding cellular machineries compared to viruses with smaller genomes.

Scarcity of haloarchaeal virus isolates in the environment

The relative abundance of viruses in any particular sample or environment can be estimated by mapping the sequence reads from a metavirome to the reference genomes and expressed as **R**eads recruited **P**er **K**b of genome per **G**b of metagenome (RPKG). We used this approach to compare the relative abundance of the four viruses described in this study to that of the previously reported cultivated and uncultivated haloarchaeal viruses. To this end, we analyzed saltern viromes sequenced from Lake Retba (Roux *et al.*, 2016) and South Bay Salt Works (Rodriguez-Brito *et al.*, 2010). Notably, the samples for the preparation of the Lake Retba virome (Roux *et al.*, 2016) were collected during the same sampling trip as those used to isolate viruses reported herein. However, none of the cultivated haloarchaeal viruses, including those

described here, were sufficiently similar to the sequences present in the available viromes. By contrast, uncultured viruses predicted to infect *Haloquadratum walsbyi* recruited around 15,000 RPKG and formed a distinct clade in the phylogenomic tree (Supplementary Fig. 7). Apart from these, other uncultured viruses with no identified host and one virus predicted to infect nanohaloarchaea have recruitment of around 10 RPKG. The fact that all currently cultured viruses recruit only negligible number of reads, even when the virome originates from the same site as virus isolates is likely to reflect the still scarce and biased sampling of the (halo)archaeal virome. At least in the case of the Lake Retba viruses and the corresponding virome, the two have been isolated at the same time and thus temporal variation in virus diversity cannot explain this result. Given the low abundance of *Halorubrum* spp. in salterns from warm environments (Garcia-Heredia *et al.*, 2012), the currently used culture-based approaches appear to be biased towards isolation of viruses that represent a rather minor fraction of the natural haloarchaeal virome. We note, however, that *Halorubrum* species represent one of the dominant components of the haloarchaeal communities in the cold hypersaline environments, such as Deep Lake in Antarctica (DeMaere *et al.*, 2013); thus, *Halorubrum* viruses might specifically dominate the cold-adapted haloarchaeal viromes. To obtain further insights into the actual diversity of haloarchaeal viruses and to initiate studies on the biology of ecologically relevant virus-host systems, future work should focus on improving the cultivation protocols for the dominant inhabitants of the hypersaline environments, such as *Haloquadratum* spp. (Oh *et al.*, 2010; Dyall-Smith *et al.*, 2011). Nevertheless, further characterization of the "cultivable minority" component of the haloarchaeal virome, as described in this study, provides important insights into the general mechanisms of haloarchaeal virus evolution and might lead to the establishment of virus-host systems in genetically tractable haloarchaeal hosts, such as *Haloferax*, for in-depth studies on virus-host interactions.

Experimental Procedures

Sampling and growth conditions

Samples were collected from Lake Retba, Senegal in May, 2011 (14°50'14'' N, 17°14'55'' W). The Lake Retba sample 1 (LR1) was collected in the center of the lake, where salt was precipitated at the bottom. LR1 sample contained grey water with grey sediment mixed with salt. The Lake Retba sample 2 (LR2) consists of purple water with white salt sediment. The temperature, pH, and salinity of the water at the sampling site was measured at the time of the sampling.

Isolation of microorganisms and viruses was carried out during the summer and autumn 2011. For isolation, the liquid phase and the sediment (including precipitated salt) were separated by decanting. Water was transferred to clean bottles. The sediments were dissolved by adding of 6% SW buffer (see below) until salts dissolved at the room temperature (magnetic stirring). Liquid phase and the dissolved sediment were treated as one sample.

Strains and viruses were aerobically grown in modified growth medium (MGM) (Nuttall and Dyall-Smith, 1993) at 37 °C. For plaque assay, different dilutions of virus sample were mixed with host culture (300 µl) and melted top layer agar (3 ml) and plated on MGM plates. For plaque assay, the hosts were grown for 2-3 over nights to obtain stationary phase culture. For making of MGM, 30% saltwater (SW) containing 240 g NaCl, 30 g $MgCl_2 \times 6H_2O$, 35 g $MgSO_4 \times 7H_20$, 7 g KCl, 5 ml of 1 M $CaCl_2 \times 2H_20$, and 80 ml of 1 M Tris-HCl pH 7.2 (per liter of water) was prepared as described in the Halohandbook (Dyall-Smith, 2009). One litre of MGM medium contained 5 g of peptone (Oxoid), and 1 g of Bacto yeast extract (Becton, Dickinson and Company). Top layer, solid, and liquid medium contained 18% SW, 20% SW, and 23% SW, respectively. For the top layer and solid media, 4 g or 14 g of Bacto agar (Becton, Dickinson and Company) was added, respectively.

Isolation of microorganisms, 16S rRNA gene sequencing and phylogenetic tree

To isolate strains from the samples, aliquots of samples (100 µl) were directly plated on MGM plates and grown at 37 °C in a covered box. A selection of colonies with different morphologies and colors were picked and colony purified by streaking single colonies on solid media by three consecutive times. The archaeal strains used in the study are listed in Table 2. The strains were identified based on their partial 16S rRNA gene sequences, which were determined as described previously (Sime-Ngando *et al.*, 2011). The 16S rRNA genes were amplified by PCR. The primers were either universal for both the bacteria and archaea, or specific for the archaea (Eder *et al.*, 1999). The sequences of the universal prokaryotic forward primers were 5'-AGAGTTTGATCCTGGCTCAG-3' (F27) and 5'-TCCGTGCCAGCAGCCGCCG -3' (F530), and those of the universal prokaryotic reverse primers were 5´-ACGGHTACCTTGTTACGACTT-3' (1512uR) and 5'-CGTATTACCGCGGCTGCTGG-3' (R518). The archaea-specific primers were 5'-TCYGGTTGATCCTGCC-3' (8aF) and 5'-AGGAGGTGATCCAGCC-3' (AR1456). The reaction mixture (50 µl of total volume) contained 1X Taq™ buffer (Promega, Madison, WI, USA), 1.5 mM $MgCl_2$, dNTPs at a concentration of 0.2 mM each, 1 U of Taq polymerase, each primer at a concentration of 125 pmol, and 5 ng of template DNA. The amplification was ended by an extension step for 10 min at 72°C. Negative and positive controls were included. Five µl of PCR products were loaded onto 0.8 % agarose gel in TAE 1X (Tris-acetic acid-EDTA buffer) and visualized under UV light after ethidium bromide staining. PCR products obtained were cloned using TOPO TA cloning kit (Invitrogen, Carlsbad, CA, USA) according to the manufacturer's protocol. After blue-white selection, positive clones were grown at 37°C overnight on 96-well tissue culture plates in the presence of kanamycin.

The clones were picked and suspended in TE followed by boiling at 96°C, and used as a template DNA for PCR amplification using M13 primers targeting the cloning vector (5'-GTAAAACGACGGCCAG-3' and 5'-CAGGAAACAGCTATGAC-3'). The selected clones were grown as previously to extract plasmid DNA using Nucleospin Plasmid preparation Kit (Macherey-Nagel, EURL, France) and sent for Sanger sequencing using M13 primers on both strands. For a first classification, we used the SILVA r128 rRNA classifier (Pruesse *et al.*, 2012). For the phylogenetic tree, sequences were aligned using MUSCLE (Edgar, 2004) and maximum

likelihood trees were constructed using the program FastTree2 (Price *et al.*, 2010). Bootstrapping (100 replicates) was performed using the Seqboot program in the PHYLIP package (Felsenstein, 1993).

The sequences are deposited in the NCBI data bank under the accession numbers MG462733-MG462751 (Table 2).

Isolation of viruses

Viruses were isolated either by direct plating or enrichment culture techniques. The pure cultures of LR1 host strains (Table 2) were used to isolate viruses from LR1 samples. Hosts of LR2 (Table 2) were used to isolate viruses from LR2 samples. The LR1 and LR2 samples were first centrifuged at 13 000 rpm (Table-top Eppendorf centrifuge) for 10 min at room temperature and the supernatant we used for virus isolation. To remove microorganisms from the LR1 sediment sample, the sample was filtered (pore size 0.2 µm). For direct plating, 100 µl of samples was mixed with dense host culture (300 µl) and melted top layer agar (3 ml) and poured on a plate, which was incubated at 37 °C until a dense lawn of archaea was observed (typically two to three days). For enrichments, 500 µl of samples was mixed with host culture (1 ml grown for 2-3 days) and incubated in a shaker (200 rpm) 1-2 overnights. The enrichment samples (100 µl and 500 µl) were plated as above. The obtained plaques were plaque purified. The plaque purification was carried out by growing the viruses on their host strain to obtain separate plaques by using plaque assay. Plaques were picked by sterile toothpick or Pasteur pipette, and a single plaque was resuspended in 0.5 ml of MGM liquid medium. The plaque purification was repeated by using the single plaque as the starting material. The single plaque purification was carried out by three consecutive times for each virus.

For all plaque assays and preparation of the virus stocks, appropriate virus dilution (100 µl) mixed with host culture (300 µl) and melted top layer agar (3 ml) was plated. The plates were incubated for 2-3 days. The virus stocks were prepared from semiconfluent plates. Top layer media from the semiconfluent plates were collected by a sterile glass triangle into a sterile Erlenmeyer bottle and 2 ml of liquid medium was added per each collected plate. The suspension was incubated for 1.5 hours at 37 °C. Cell debris and agar were

removed by centrifugation (Thermo Scientific F12 rotor, 8000 rpm, 20 min, 5 °C). The supernatant was put into a clean bottle and it is referred as a virus stock. One semiconfluent plate produces approximately 3-3.5 ml of virus stock. Stability of viruses (virus stocks stored at 4 °C) was monitored for four weeks by plaque assay. To test the sensitivity of the viruses to organic solvents and detergents, viruses (virus stock in MGM) were incubated in 20% (v/v) chloroform, 0.1% (v/v) Nonidet P-40, or 0.1% Triton X-100 for 15 min at 22°C. MGM was used as a control. The infectivity of the viruses was determined by plaque assay and the experiments have been repeated at least for two times.

Virus purification and particle analysis

The virus stocks (typically made of 200 plates producing 600-700 ml of virus stock or 400 plates producing 1200-1400 ml of virus stock) were treated with DNase I (70 µg/ml; 30 min at 37 °C; Sigma-Aldrich) prior the purification. Viruses were precipitated from the virus stocks by using two-step polyethylene glycol (PEG)-NaCl precipitation (Yamamoto *et al.*, 1970). First, the impurities were precipitated by using 4% (w/v) PEG 6000 (no NaCl added due to the high salinity of the virus stock). PEG was dissolved by magnetic stirring for 30 min at 4°C. After centrifugation (Thermo Scientific F12 rotor, 8000 rpm, 40 min, 5 °C), PEG was added to the supernatant to obtain a final concentration of 11% (w/v). After dissolution of PEG and centrifugation (see above), the obtained virus precipitate was dissolved in 18% SW buffer followed by removal of the aggregates and undissolved components (Thermo Scientific F20 rotor, 7000 rpm, 10 min, 5 °C). Viruses were first purified by rate zonal ultracentrifugation in sucrose by using linear 5-20% sucrose gradients (18% SW buffer; Sorvall rotor AH629, 24 000 rpm, 15 °C). The running times were 2.5 h (HRPV10), 1 h 45 min (HRPV11), and 3 h (HRPV12 and HFTV1). After rate zonal centrifugation, viruses were purified by equilibrium centrifugation in CsCl gradients (mean ρ=1.30-1.35 g/ml in 18% SW; Sorvall rotor AH629, 20 000 rpm, 19 h, 20 °C), and concentrated by differential centrifugation (Sorvall rotor T647.5, 32 000 rpm, 3-5 h, 15 °C). Virus purifications were repeated at least three times for each virus. Protein concentrations were determined by Bradford assay using bovine serum albumin as a standard (Bradford, 1976). The

proteins were analyzed by using modified tricine-sodium dodecyl sulfate polyacrylamide gel electrophoresis (14% acrylamide in the separation gel; (Schägger and von Jagow, 1987)). Gels were stained with Coomassie Brilliant Blue R 250 (Serva).

Viral lipids were isolated by chloroform-methanol extraction from the purified HRPV10, HRPV11, and HRPV12 virus particles and from the early-stationary-phase cells of *Haloarcula hispanica* (Juez *et al.*, 1986) and *Halorubrum* sp. LR2-17, LR2-12, LR1-23 strains as previously described (Folch *et al.*, 1957; Kates *et al.*, 1972). Extracted lipids were dissolved in chloroform-methanol (9:1) and analyzed on pre-activated thin layer chromatography (TLC) silica plates, which were developed with chloroform–methanol–90% acetic acid (65:4:35 [vol/vol/vol]). Lipids were visualized by ammonium molybdate staining (Arnold *et al.*, 2000). The plate was quickly dipped into a solution containing 10% (v/v) H_2SO_4 and 5% (w/v) ammonium molybdate, after which the excess liquid was dried, and the plate was incubated at 140 °C for around 15 min.

For transmission electron microscopy, 5 µl samples of the purified virus particles were adsorbed on copper pioloform coated grids (Electron Microscopy Unit, HiLIFE Institute of Biotechnology, University of Helsinki). The particles were negatively stained either with 3% (w/v) uranylacetate (pH 4.5) or 1% (w/v) phosphotungstic acid (pH 7.0) , and visualized by JEOL 1400 transmission electron microscope (Electron Microscopy Unit, HiLIFE Institute of Biotechnology, University of Helsinki) operating at 80 kV acceleration voltage.

Virus genome analysis, sequencing and annotation

Nucleic acid was purified from the pure virus particles. The particles in 18% SW were diluted 1:4 in 20 mM Tris-HCl, pH 7.2 and treated with 1% (w/v) sodium dodecyl sulphate and 100 µg/ml proteinase K (Thermo Scientific) in the presence of 1 mM ethylenediaminetetraacetic acid (EDTA) for an hour at 37 °C. Nucleic acid was extracted by phenol-ether extraction and followed by precipitation with NaCl and ethanol. Purified nucleic acids were treated with RQ1 DNase (Promega), Exonuclease III (Fermentas), Mung bean nuclease (MBN 0.025, 0.5, or 5.0 U/µg DNA; Promega) according to manufacturers' instructions. For MBN

experiments, phage ϕX174 ssDNA genome and its dsDNA replicative form RFII (New England Biolabs) were used as controls.

Libraries were prepared using TruSeq PCRfree library preparation. Samples were sequenced by Illumina MiSeq 600 cycles (Illumina Inc., San Diego, CA) with 2x300 bp read length. The sequencing reads were trimmed based on the quality scores (limit 0.05) from a base-caller algorithm available in the sequencing files. The trimming was performed using the modified-Mott trimming algorithm implemented in the CLC Genomics Workbench v7 (QIAGEN Bioinformatics) and the trimmed reads were subsequently assembled into contigs using the same software with default parameters. Protein-coding genes were predicted using Prodigal (Hyatt *et al.*, 2010), and tRNA genes using tRNAscan-SE (Lowe and Eddy, 1997). Additional annotation of genes was done by comparing against the NCBI NR, COG (Tatusov *et al.*, 2003), and TIGRfam (Haft *et al.*, 2001) databases, and also manually annotated using HHPRED server (Zimmermann *et al.*, 2018). The sequences are deposited in the NCBI GenBank data bank under the accession numbers MG550110 - MG550113.

All pairwise comparisons of the nucleotide sequences were conducted using the Genome-BLAST Distance Phylogeny (GBDP) method (Meier-Kolthoff *et al.*, 2013) under settings recommended for prokaryotic viruses (Meier-Kolthoff and Goker, 2017). All reference genomes were downloaded from https://www.ncbi.nlm.nih.gov/genome/browse/

Genome phylogenies were constructed using VICTOR (Meier-Kolthoff and Goker, 2017), a Genome BLAST Distance Phylogeny (GBDP) method which calculates intergenomic distances between pairs of viruses based on pairwise comparison of nucleotide sequences. The resulting intergenomic distances (including 100 replicates each) were used to infer a balanced minimum evolution tree with branch support via FASTME including SPR postprocessing (Lefort *et al.*, 2015) for the formula D0. The trees were rooted at the outgroup and visualized with FigTree (Rambaut, 2006). For both single gene phylogenies, the sequences were aligned using MUSCLE (Edgar, 2004). Maximum likelihood trees were constructed using the program FastTree2 (Price *et al.*, 2010). Bootstrapping was performed using the Seqboot program in the PHYLIP

package (Felsenstein, 1993). Comparisons among related viral genomes and reference genomes were performed using tBLASTx or BLASTN (Edgar, 2010).

Virus-host interaction studies

Infectivity of HRPV10, HRPV11, HRPV12, and HFTV1 viruses was tested on 19 Lake Retba strains (Table 2) and 48 culture collection strains representing genus *Halorubrum* or *Haloferax* (Supplementary Table 3) by spot-on-lawn assay. Undiluted and diluted (10^{-2}) virus stocks (10 µl) were applied on the top layer agar inoculated with the test strain. The virus host strain and MGM medium were used as positive and negative controls. All positive results (growth inhibitions) were verified by plaque assay.

Analysis of metaviromes

Viromes were downloaded from Metavir 2 (Roux *et al.*, 2014). Only sequence matches longer than 50 bp withe-value less than 1e-5 and more than 95% identity were considered. The recruitment of each genome from the virome was calculated by dividing the number of hits by the length of the contig (in kb) and by the size of the database (in Gb). This normalized measure is abbreviated as RPKG (**R**eads recruited **P**er **K**b of genome per **G**b of metagenome).

In order to test the performance of the currently available tools for identifying archaeal viruses in metagenomic dataset, we ran the VirSorter analysis (Roux *et al.*, 2015) against the RefSeq virus database. Of the four genomes analyzed, only HFTV1 was considered by VirSorter to be of viral origin under the category 2 (“quite sure”), with three detected “phage hallmark genes”. None of the pleolipoviruses was recognized as a virus, pointing to a need for improvement of the database of virus hallmark genes.

Acknowledgments

This work was partly supported by Agence Nationale pour la Recherche grant #ANR-17-CE15-0005-01 (project ENVIRA) to MK and the European Research Council (ERC) grant from the European Union's Seventh Framework Program (FP/2007-2013)/Project EVOMOBIL-ERC Grant Agreement no. 340440 to PF. CMM was supported by the European Molecular Biology Organization (ALTF 1562-2015) and Marie Curie Actions program from the European Commission (LTFCOFUND2013, GA-2013-609409). The use of the facilities and expertise of the Instruct-HiLIFE Biocomplex unit (Instruct Centre for Virus Production 2009-2017), member of Instruct-FI, is gratefully acknowledged. Academy of Finland and University of Helsinki are acknowledged for the support for the Instruct-FI. We thank Sari Korhonen and Soile Storman for skilled technical assistance and Mirka Lampi for help in virus purification. We are also grateful to Ying Liu for her help with HFTV1 genome annotation.

The authors have no conflict of interest to declare.

References

Aalto, A.P., Bitto, D., Ravantti, J.J., Bamford, D.H., Huiskonen, J.T., and Oksanen, H.M. (2012) Snapshot of virus evolution in hypersaline environments from the characterization of a membrane-containing Salisaeta icosahedral phage 1. *Proc Natl Acad Sci U S A* **109**: 7079-7084.

Abby, S.S., Melcher, M., Kerou, M., Krupovic, M., Stieglmeier, M., Rossel, C. *et al.* (2018) Candidatus Nitrosocaldus cavascurensis, an ammonia oxidizing, extremely thermophilic archaeon with a highly mobile genome. *Front Microbiol* **9**: 28.

Abrescia, N.G., Bamford, D.H., Grimes, J.M., and Stuart, D.I. (2012) Structure unifies the viral universe. *Annu Rev Biochem* **81**: 795-822.

Ahlgren, N.A., Fuchsman, C.A., Rocap, G., and Fuhrman, J.A. (2019) Discovery of several novel, widespread, and ecologically distinct marine Thaumarchaeota viruses that encode amoC nitrification genes. *ISME J*: [Epub ahead of print].

Arnold, H.P., Zillig, W., Ziese, U., Holz, I., Crosby, M., Utterback, T. *et al.* (2000) A novel lipothrixvirus, SIFV, of the extremely thermophilic crenarchaeon Sulfolobus. *Virology* **267**: 252-266.

Atanasova, N.S., Bamford, D.H., and Oksanen, H.M. (2015a) Haloarchaeal virus morphotypes. *Biochimie* **118**: 333-343.

Atanasova, N.S., Oksanen, H.M., and Bamford, D.H. (2015b) Haloviruses of archaea, bacteria, and eukaryotes. *Curr Opin Microbiol* **25**: 40-48.

Atanasova, N.S., Roine, E., Oren, A., Bamford, D.H., and Oksanen, H.M. (2012) Global network of specific virus-host interactions in hypersaline environments. *Environ Microbiol* **14**: 426-440.

Atanasova, N.S., Demina, T.A., Buivydas, A., Bamford, D.H., and Oksanen, H.M. (2015c) Archaeal viruses multiply: temporal screening in a solar saltern. *Viruses* **7**: 1902-1926.

Atanasova, N.S., Demina, T.A., Krishnam Rajan Shanthi, S.N.V., Oksanen, H.M., and Bamford, D.H. (2018a) Extremely halophilic pleomorphic archaeal virus HRPV9 extends the diversity of pleolipoviruses with integrases. *Res Microbiol* **169**: 500-504.

Atanasova, N.S., Heiniö, C.H., Demina, T.A., Bamford, D.H., and Oksanen, H.M. (2018b) The unexplored diversity of pleolipoviruses: the surprising case of two viruses with identical major structural modules. *Genes (Basel)* **9**: 131.

Bamford, D.H., Pietilä, M.K., Roine, E., Atanasova, N.S., Dienstbier, A., Oksanen, H.M., and ICTV Report Consortium (2017) ICTV Virus Taxonomy Profile: Pleolipoviridae. *J Gen Virol* **98**: 2916-2917.

Bamford, D.H., Ravantti, J.J., Rönnholm, G., Laurinavicius, S., Kukkaro, P., Dyall-Smith, M. *et al.* (2005) Constituents of SH1, a novel lipid-containing virus infecting the halophilic euryarchaeon Haloarcula hispanica. *J Virol* **79**: 9097-9107.

Bankevich, A., Nurk, S., Antipov, D., Gurevich, A.A., Dvorkin, M., Kulikov, A.S. *et al.* (2012) SPAdes: a new genome assembly algorithm and its applications to single-cell sequencing. *J Comput Biol* **19**: 455-477.

Bell, S.D., and Botchan, M.R. (2013) The minichromosome maintenance replicative helicase. *Cold Spring Harb Perspect Biol* **5**: a012807.

Bradford, M.M. (1976) A rapid and sensitive method for the quantitation of microgram quantities of protein utilizing the principle of protein-dye binding. *Anal Biochem* **72**: 248-254.

Crits-Christoph, A., Gelsinger, D.R., Ma, B., Wierzchos, J., Ravel, J., Davila, A. *et al.* (2016) Functional interactions of archaea, bacteria and viruses in a hypersaline endolithic community. *Environ Microbiol* **18**: 2064-2077.

Cuadros-Orellana, S., Martin-Cuadrado, A.B., Legault, B., D'Auria, G., Zhaxybayeva, O., Papke, R.T., and Rodriguez-Valera, F. (2007) Genomic plasticity in prokaryotes: the case of the square haloarchaeon. *ISME J* **1**: 235-245.

Danovaro, R., Dell'Anno, A., Corinaldesi, C., Rastelli, E., Cavicchioli, R., Krupovic, M. *et al.* (2016) Virus-mediated archaeal hecatomb in the deep seafloor. *Sci Adv* **2**: e1600492.

De Paepe, M., Hutinet, G., Son, O., Amarir-Bouhram, J., Schbath, S., and Petit, M.A. (2014) Temperate phages acquire DNA from defective prophages by relaxed homologous recombination: the role of Rad52-like recombinases. *PLoS Genet* **10**: e1004181.

DeMaere, M.Z., Williams, T.J., Allen, M.A., Brown, M.V., Gibson, J.A., Rich, J. *et al.* (2013) High level of intergenera gene exchange shapes the evolution of haloarchaea in an isolated Antarctic lake. *Proc Natl Acad Sci U S A* **110**: 16939-16944.

Demina, T.A., Atanasova, N.S., Pietilä, M.K., Oksanen, H.M., and Bamford, D.H. (2016a) Vesicle-like virion of Haloarcula hispanica pleomorphic virus 3 preserves high infectivity in saturated salt. *Virology* **499**: 40-51.

Demina, T.A., Pietilä, M.K., Svirskaite, J., Ravantti, J.J., Atanasova, N.S., Bamford, D.H., and Oksanen, H.M. (2016b) Archaeal Haloarcula californiae icosahedral virus 1 highlights conserved elements in icosahedral membrane-containing DNA viruses from extreme environments. *mBio* **7**.

Demina, T.A., Pietilä, M.K., Svirskaite, J., Ravantti, J.J., Atanasova, N.S., Bamford, D.H., and Oksanen, H.M. (2017) HCIV-1 and other tailless icosahedral internal membrane-containing viruses of the family Sphaerolipoviridae. *Viruses* **9**.

Di Meglio, L., Santos, F., Gomariz, M., Almansa, C., Lopez, C., Anton, J., and Nercessian, D. (2016) Seasonal dynamics of extremely halophilic microbial communities in three Argentinian salterns. *FEMS Microbiol Ecol* **92**.

Dyall-Smith, M. (2009). Halohandbook. URL http://www.haloarchaea.com/resources/halohandbook/

Dyall-Smith, M., and Pfeiffer, F. (2018) The PL6-family plasmids of Haloquadratum are virus-related. *Front Microbiol* **9**: 1070.

Dyall-Smith, M., Pfeifer, F., Witte, A., Oesterhelt, D., and Pfeiffer, F. (2018) Complete genome sequence of the model halovirus phiH1 (phiH1). *Genes (Basel)* **9**.

Dyall-Smith, M., Palm, P., Wanner, G., Witte, A., Oesterhelt, D., and Pfeiffer, F. (2019) Halobacterium salinarum virus ChaoS9, a Novel Halovirus Related to PhiH1 and PhiCh1. *Genes (Basel)* **10**.

Dyall-Smith, M.L., Pfeiffer, F., Klee, K., Palm, P., Gross, K., Schuster, S.C. *et al.* (2011) *Haloquadratum walsbyi*: limited diversity in a global pond. *PLoS One* **6**: e20968.

Eder, W., Ludwig, W., and Huber, R. (1999) Novel 16S rRNA gene sequences retrieved from highly saline brine sediments of kebrit deep, red Sea. *Arch Microbiol* **172**: 213-218.

Edgar, R.C. (2004) MUSCLE: multiple sequence alignment with high accuracy and high throughput. *Nucleic Acids Res* **32**: 1792-1797.

Edgar, R.C. (2010) Search and clustering orders of magnitude faster than BLAST. *Bioinformatics* **26**: 2460-2461.

El Omari, K., Li, S., Kotecha, A., Walter, T.S., Bignon, E.A., Harlos, K. *et al.* (2019) The structure of a prokaryotic viral envelope protein expands the landscape of membrane fusion proteins. *Nat Commun* **10**: 846.

Erdmann, S., Tschitschko, B., Zhong, L., Raftery, M.J., and Cavicchioli, R. (2017) A plasmid from an Antarctic haloarchaeon uses specialized membrane vesicles to disseminate and infect plasmid-free cells. *Nat Microbiol* **2**: 1446-1455.

Felsenstein, J. (1993) *PHYLIP (phylogeny inference package), version 3.5 c*: Joseph Felsenstein.

Folch, J., Lees, M., and Sloane Stanley, G.H. (1957) A simple method for the isolation and purification of total lipides from animal tissues. *J Biol Chem* **226**: 497-509.

Forterre, P., Krupovic, M., Raymann, K., and Soler, N. (2014) Plasmids from Euryarchaeota. *Microbiol Spectr* **2**: PLAS-0027-2014.

Garcia-Heredia, I., Martin-Cuadrado, A.B., Mojica, F.J., Santos, F., Mira, A., Anton, J., and Rodriguez-Valera, F. (2012) Reconstructing viral genomes from the environment using fosmid clones: the case of haloviruses. *PLoS One* **7**: e33802.

Gardner, A.F., Bell, S.D., White, M.F., Prangishvili, D., and Krupovic, M. (2014) Protein-protein interactions leading to recruitment of the host DNA sliding clamp by the hyperthermophilic Sulfolobus islandicus rod-shaped virus 2. *J Virol* **88**: 7105-7108.

Garneau, J.R., Depardieu, F., Fortier, L.C., Bikard, D., and Monot, M. (2017) PhageTerm: a tool for fast and accurate determination of phage termini and packaging mechanism using next-generation sequencing data. *Sci Rep* **7**: 8292.

Gunde-Cimerman, N., Plemenitas, A., and Oren, A. (2018) Strategies of adaptation of microorganisms of the three domains of life to high salt concentrations. *FEMS Microbiol Rev* **42**: 353-375.

Haft, D.H., Loftus, B.J., Richardson, D.L., Yang, F., Eisen, J.A., Paulsen, I.T., and White, O. (2001) TIGRFAMs: a protein family resource for the functional identification of proteins. *Nucleic Acids Res* **29**: 41-43.

Hyatt, D., Chen, G.L., Locascio, P.F., Land, M.L., Larimer, F.W., and Hauser, L.J. (2010) Prodigal: prokaryotic gene recognition and translation initiation site identification. *BMC Bioinformatics* **11**: 119.

Iranzo, J., Krupovic, M., and Koonin, E.V. (2016a) The double-stranded DNA virosphere as a modular hierarchical network of gene sharing. *mBio* **7**: e00978-00916.

Iranzo, J., Koonin, E.V., Prangishvili, D., and Krupovic, M. (2016b) Bipartite network analysis of the archaeal virosphere: evolutionary connections between viruses and capsidless mobile elements. *J Virol* **90**: 11043-11055.

Juez, G., Rodriguez-Valera, F., Ventosa, A., and Kushner, D.J. (1986) Haloarcula hispanica spec. nov. and Haloferax gibbonsii spec, nov., two new species of extremely halophilic archaebacteria. *Syst Appl Microbiol* **8**: 75-79.

Juhala, R.J., Ford, M.E., Duda, R.L., Youlton, A., Hatfull, G.F., and Hendrix, R.W. (2000) Genomic sequences of bacteriophages HK97 and HK022: pervasive genetic mosaicism in the lambdoid bacteriophages. *J Mol Biol* **299**: 27-51.

Kates, M., Work, T.S., and Work, E. (1972) *Techniques of Lipidology: Isolation, Analysis and Identification of Lipids*. North-Holland, Amsterdam.

Kazlauskas, D., Krupovic, M., and Venclovas, C. (2016) The logic of DNA replication in double-stranded DNA viruses: insights from global analysis of viral genomes. *Nucleic Acids Res* **44**: 4551-4564.

Koskella, B., Thompson, J.N., Preston, G.M., and Buckling, A. (2011) Local biotic environment shapes the spatial scale of bacteriophage adaptation to bacteria. *Am Nat* **177**: 440-451.

Krupovic, M., and Bamford, D.H. (2010) Order to the viral universe. *J Virol* **84**: 12476-12479.

Krupovic, M., Forterre, P., and Bamford, D.H. (2010a) Comparative analysis of the mosaic genomes of tailed archaeal viruses and proviruses suggests common themes for virion architecture and assembly with tailed viruses of bacteria. *J Mol Biol* **397**: 144-160.

Krupovic, M., Gribaldo, S., Bamford, D.H., and Forterre, P. (2010b) The evolutionary history of archaeal MCM helicases: a case study of vertical evolution combined with hitchhiking of mobile genetic elements. *Mol Biol Evol* **27**: 2716-2732.

Krupovic, M., Prangishvili, D., Hendrix, R.W., and Bamford, D.H. (2011a) Genomics of bacterial and archaeal viruses: dynamics within the prokaryotic virosphere. *Microbiol Mol Biol Rev* **75**: 610-635.

Krupovic, M., Spang, A., Gribaldo, S., Forterre, P., and Schleper, C. (2011b) A thaumarchaeal provirus testifies for an ancient association of tailed viruses with archaea. *Biochem Soc Trans* **39**: 82-88.

Krupovic, M., Cvirkaite-Krupovic, V., Iranzo, J., Prangishvili, D., and Koonin, E.V. (2018) Viruses of archaea: structural, functional, environmental and evolutionary genomics. *Virus Res* **244**: 181-193.

Lefort, V., Desper, R., and Gascuel, O. (2015) FastME 2.0: A Comprehensive, Accurate, and Fast Distance-Based Phylogeny Inference Program. *Mol Biol Evol* **32**: 2798-2800.

Li, M., Liu, H., Han, J., Liu, J., Wang, R., Zhao, D. *et al.* (2013) Characterization of CRISPR RNA biogenesis and Cas6 cleavage-mediated inhibition of a provirus in the haloarchaeon Haloferax mediterranei. *J Bacteriol* **195**: 867-875.

Liu, Y., Wang, J., Liu, Y., Wang, Y., Zhang, Z., Oksanen, H.M. *et al.* (2015) Identification and characterization of SNJ2, the first temperate pleolipovirus integrating into the genome of the SNJ1-lysogenic archaeal strain. *Mol Microbiol* **98**: 1002-1020.

Lopes, A., Amarir-Bouhram, J., Faure, G., Petit, M.A., and Guerois, R. (2010) Detection of novel recombinases in bacteriophage genomes unveils Rad52, Rad51 and Gp2.5 remote homologs. *Nucleic Acids Res* **38**: 3952-3962.

Lopez-Perez, M., Haro-Moreno, J.M., de la Torre, J.R., and Rodriguez-Valera, F. (2019) Novel Caudovirales associated with Marine Group I Thaumarchaeota assembled from metagenomes. *Environ Microbiol*: [Epub ahead of print].

Lowe, T.M., and Eddy, S.R. (1997) tRNAscan-SE: a program for improved detection of transfer RNA genes in genomic sequence. *Nucleic Acids Res* **25**: 955-964.

Maier, L.K., Dyall-Smith, M., and Marchfelder, A. (2015) The adaptive immune system of *Haloferax volcanii*. *Life (Basel)* **5**: 521-537.

Makarova, K.S., Wolf, Y.I., Forterre, P., Prangishvili, D., Krupovic, M., and Koonin, E.V. (2014) Dark matter in archaeal genomes: a rich source of novel mobile elements, defense systems and secretory complexes. *Extremophiles* **18**: 877-893.

Meier-Kolthoff, J.P., and Goker, M. (2017) VICTOR: genome-based phylogeny and classification of prokaryotic viruses. *Bioinformatics* **33**: 3396-3404.

Meier-Kolthoff, J.P., Auch, A.F., Klenk, H.P., and Goker, M. (2013) Genome sequence-based species delimitation with confidence intervals and improved distance functions. *BMC Bioinformatics* **14**: 60.

Mizuno, C.M., Rodriguez-Valera, F., Kimes, N.E., and Ghai, R. (2013) Expanding the marine virosphere using metagenomics. *PLoS Genet* **9**: e1003987.

Nuttall, S.D., and Dyall-Smith, M.L. (1993) HF1 and HF2: novel bacteriophages of halophilic archaea. *Virology* **197**: 678-684.

Oh, D., Porter, K., Russ, B., Burns, D., and Dyall-Smith, M. (2010) Diversity of Haloquadratum and other haloarchaea in three, geographically distant, Australian saltern crystallizer ponds. *Extremophiles* **14**: 161-169.

Oren, A. (2002) Molecular ecology of extremely halophilic Archaea and Bacteria. *FEMS Microbiol Ecol* **39**: 1-7.

Oren, A., Bratbak, G., and Heldal, M. (1997) Occurrence of virus-like particles in the Dead Sea. *Extremophiles* **1**: 143-149.

Pagaling, E., Haigh, R.D., Grant, W.D., Cowan, D.A., Jones, B.E., Ma, Y. *et al.* (2007) Sequence analysis of an Archaeal virus isolated from a hypersaline lake in Inner Mongolia, China. *BMC Genomics* **8**: 410.

Pan, M., Kelman, L.M., and Kelman, Z. (2011) The archaeal PCNA proteins. *Biochem Soc Trans* **39**: 20-24.

Pedulla, M.L., Ford, M.E., Houtz, J.M., Karthikeyan, T., Wadsworth, C., Lewis, J.A. *et al.* (2003) Origins of highly mosaic mycobacteriophage genomes. *Cell* **113**: 171-182.

Philosof, A., Yutin, N., Flores-Uribe, J., Sharon, I., Koonin, E.V., and Beja, O. (2017) Novel abundant oceanic viruses of uncultured Marine Group II Euryarchaeota. *Curr Biol* **27**: 1362-1368.

Pietilä, M.K., Atanasova, N.S., Oksanen, H.M., and Bamford, D.H. (2013a) Modified coat protein forms the flexible spindle-shaped virion of haloarchaeal virus His1. *Environ Microbiol* **15**: 1674-1686.

Pietilä, M.K., Roine, E., Paulin, L., Kalkkinen, N., and Bamford, D.H. (2009) An ssDNA virus infecting archaea: a new lineage of viruses with a membrane envelope. *Mol Microbiol* **72**: 307-319.

Pietilä, M.K., Laurinavicius, S., Sund, J., Roine, E., and Bamford, D.H. (2010) The single-stranded DNA genome of novel archaeal virus halorubrum pleomorphic virus 1 is enclosed in the envelope decorated with glycoprotein spikes. *J Virol* **84**: 788-798.

Pietilä, M.K., Demina, T.A., Atanasova, N.S., Oksanen, H.M., and Bamford, D.H. (2014) Archaeal viruses and bacteriophages: comparisons and contrasts. *Trends Microbiol* **22**: 334-344.

Pietilä, M.K., Roine, E., Sencilo, A., Bamford, D.H., and Oksanen, H.M. (2016) Pleolipoviridae, a newly proposed family comprising archaeal pleomorphic viruses with single-stranded or double-stranded DNA genomes. *Arch Virol* **161**: 249-256.

Pietilä, M.K., Atanasova, N.S., Manole, V., Liljeroos, L., Butcher, S.J., Oksanen, H.M., and Bamford, D.H. (2012) Virion architecture unifies globally distributed pleolipoviruses infecting halophilic archaea. *J Virol* **86**: 5067-5079.

Pietilä, M.K., Laurinmäki, P., Russell, D.A., Ko, C.C., Jacobs-Sera, D., Hendrix, R.W. *et al.* (2013b) Structure of the archaeal head-tailed virus HSTV-1 completes the HK97 fold story. *Proc Natl Acad Sci U S A* **110**: 10604-10609.

Pietilä, M.K., Laurinmäki, P., Russell, D.A., Ko, C.C., Jacobs-Sera, D., Butcher, S.J. *et al.* (2013c) Insights into head-tailed viruses infecting extremely halophilic archaea. *J Virol* **87**: 3248-3260.

Pope, W.H., Bowman, C.A., Russell, D.A., Jacobs-Sera, D., Asai, D.J., Cresawn, S.G. *et al.* (2015) Whole genome comparison of a large collection of mycobacteriophages reveals a continuum of phage genetic diversity. *Elife* **4**: e06416.

Prangishvili, D., Bamford, D.H., Forterre, P., Iranzo, J., Koonin, E.V., and Krupovic, M. (2017) The enigmatic archaeal virosphere. *Nat Rev Microbiol* **15**: 724-739.

Price, M.N., Dehal, P.S., and Arkin, A.P. (2010) FastTree 2--approximately maximum-likelihood trees for large alignments. *PLoS One* **5**: e9490.

Pruesse, E., Peplies, J., and Glockner, F.O. (2012) SINA: accurate high-throughput multiple sequence alignment of ribosomal RNA genes. *Bioinformatics* **28**: 1823-1829.

Rambaut, A. (2006) FigTree 1.4.3 - a graphical viewer of phylogenetic trees and a program for producing publication-ready figures. In *http://treebioedacuk/software/figtree/*.

Raymann, K., Forterre, P., Brochier-Armanet, C., and Gribaldo, S. (2014) Global phylogenomic analysis disentangles the complex evolutionary history of DNA replication in archaea. *Genome Biol Evol* **6**: 192-212.

Rodriguez-Brito, B., Li, L., Wegley, L., Furlan, M., Angly, F., Breitbart, M. *et al.* (2010) Viral and microbial community dynamics in four aquatic environments. *ISME J* **4**: 739-751.

Rossler, N., Klein, R., Scholz, H., and Witte, A. (2004) Inversion within the haloalkaliphilic virus phi Ch1 DNA results in differential expression of structural proteins. *Mol Microbiol* **52**: 413-426.

Roux, S., Enault, F., Hurwitz, B.L., and Sullivan, M.B. (2015) VirSorter: mining viral signal from microbial genomic data. *PeerJ* **3**: e985.

Roux, S., Tournayre, J., Mahul, A., Debroas, D., and Enault, F. (2014) Metavir 2: new tools for viral metagenome comparison and assembled virome analysis. *BMC Bioinformatics* **15**: 76.

Roux, S., Enault, F., Ravet, V., Colombet, J., Bettarel, Y., Auguet, J.C. *et al.* (2016) Analysis of metagenomic data reveals common features of halophilic viral communities across continents. *Environ Microbiol* **18**: 889-903.

Santos-Perez, I., Charro, D., Gil-Carton, D., Azkargorta, M., Elortza, F., Bamford, D.H. *et al.* (2019) Structural basis for assembly of vertical single beta-barrel viruses. *Nat Commun* **10**: 1184.

Schägger, H., and von Jagow, G. (1987) Tricine-sodium dodecyl sulfate-polyacrylamide gel electrophoresis for the separation of proteins in the range from 1 to 100 kDa. *Anal Biochem* **166**: 368-379.

Sencilo, A., Paulin, L., Kellner, S., Helm, M., and Roine, E. (2012) Related haloarchaeal pleomorphic viruses contain different genome types. *Nucleic Acids Res* **40**: 5523-5534.
Sencilo, A., Jacobs-Sera, D., Russell, D.A., Ko, C.C., Bowman, C.A., Atanasova, N.S. *et al.* (2013) Snapshot of haloarchaeal tailed virus genomes. *RNA Biol* **10**: 803-816.
Sime-Ngando, T., Lucas, S., Robin, A., Tucker, K.P., Colombet, J., Bettarel, Y. *et al.* (2011) Diversity of virus-host systems in hypersaline Lake Retba, Senegal. *Environ Microbiol* **13**: 1956-1972.
Svirskaite, J., Oksanen, H.M., Daugelavicius, R., and Bamford, D.H. (2016) Monitoring physiological changes in haloarchaeal cell during virus release. *Viruses* **8**: 59.
Söding, J., Biegert, A., and Lupas, A.N. (2005) The HHpred interactive server for protein homology detection and structure prediction. *Nucleic Acids Res* **33**: W244-248.
Tang, S.L., Nuttall, S., and Dyall-Smith, M. (2004) Haloviruses HF1 and HF2: evidence for a recent and large recombination event. *J Bacteriol* **186**: 2810-2817.
Tatusov, R.L., Fedorova, N.D., Jackson, J.D., Jacobs, A.R., Kiryutin, B., Koonin, E.V. *et al.* (2003) The COG database: an updated version includes eukaryotes. *BMC Bioinformatics* **4**: 41.
Triantaphyllidis, G.V., Abatzopoulos, T.J., and Sorgeloos, P. (1998) Review of the biogeography of the genus Artemia (Crustacea, Anostraca). *Journal of Biogeography* **25**: 213-226.
Tschitschko, B., Erdmann, S., DeMaere, M.Z., Roux, S., Panwar, P., Allen, M.A. *et al.* (2018) Genomic variation and biogeography of Antarctic haloarchaea. *Microbiome* **6**: 113.
Wang, J., Liu, Y., Liu, Y., Du, K., Xu, S., Wang, Y. *et al.* (2018a) A novel family of tyrosine integrases encoded by the temperate pleolipovirus SNJ2. *Nucleic Acids Res* **46**: 2521-2536.
Wang, Y., Chen, B., Cao, M., Sima, L., Prangishvili, D., Chen, X., and Krupovic, M. (2018b) Rolling-circle replication initiation protein of haloarchaeal sphaerolipovirus SNJ1 is homologous to bacterial transposases of the IS91 family insertion sequences. *J Gen Virol* **99**: 416-421.
Weitz, J.S., Poisot, T., Meyer, J.R., Flores, C.O., Valverde, S., Sullivan, M.B., and Hochberg, M.E. (2013) Phage-bacteria infection networks. *Trends Microbiol* **21**: 82-91.
Ventosa, A., de la Haba, R.R., Sanchez-Porro, C., and Papke, R.T. (2015) Microbial diversity of hypersaline environments: a metagenomic approach. *Curr Opin Microbiol* **25**: 80-87.
Wichels, A., Biel, S.S., Gelderblom, H.R., Brinkhoff, T., Muyzer, G., and Schutt, C. (1998) Bacteriophage diversity in the North Sea. *Appl Environ Microbiol* **64**: 4128-4133.
Vik, D.R., Roux, S., Brum, J.R., Bolduc, B., Emerson, J.B., Padilla, C.C. *et al.* (2017) Putative archaeal viruses from the mesopelagic ocean. *PeerJ* **5**: e3428.
Villamor, J., Ramos-Barbero, M.D., Gonzalez-Torres, P., Gabaldon, T., Rossello-Mora, R., Meseguer, I. *et al.* (2018) Characterization of ecologically diverse viruses infecting co-occurring strains of cosmopolitan hyperhalophilic Bacteroidetes. *ISME J* **12**: 424-437.
Vos, M., Birkett, P.J., Birch, E., Griffiths, R.I., and Buckling, A. (2009) Local adaptation of bacteriophages to their bacterial hosts in soil. *Science* **325**: 833.
Yamamoto, K.R., Alberts, B.M., Benzinger, R., Lawhorne, L., and Treiber, G. (1970) Rapid bacteriophage sedimentation in the presence of polyethylene glycol and its application to large-scale virus purification. *Virology* **40**: 734-744.
Yutin, N., Backstrom, D., Ettema, T.J.G., Krupovic, M., and Koonin, E.V. (2018) Vast diversity of prokaryotic virus genomes encoding double jelly-roll major capsid proteins uncovered by genomic and metagenomic sequence analysis. *Virol J* **15**: 67.
Zhang, Z., Liu, Y., Wang, S., Yang, D., Cheng, Y., Hu, J. *et al.* (2012) Temperate membrane-containing halophilic archaeal virus SNJ1 has a circular dsDNA genome identical to that of plasmid pHH205. *Virology* **434**: 233-241.
Zimmermann, L., Stephens, A., Nam, S.Z., Rau, D., Kubler, J., Lozajic, M. *et al.* (2018) A completely reimplemented MPI bioinformatics toolkit with a new HHpred server at its core. *J Mol Biol* **430**: 2237-2243.

Table and Figure legends

Table 1. Viruses from Lake Retba

Table 2. Strains isolated from the Lake Retba samples

Table 3. Virus purification by PEG-NaCl precipitation, rate zonal, equilibrium and differential ultracentrifugation

Figure 1. Maximum likelihood phylogenetic tree of the isolated Lake Retba strains based on the partial 16S rRNA gene sequences. Isolates from Lake Retba (LR) are highlighted in red. Sequences were aligned using MUSCLE (Edgar, 2004) and the maximum likelihood tree was constructed using the FastTree2 program (Price *et al.*, 2010). The numbers above the branches represent bootstrap support values from 100 replicates. The scale bar represents the number of substitutions per site.

Figure 2. Transmission electron microscopy of purified viruses (A) HRPV10, (B) HRPV11, (C) HRPV12 (D) HFTV1. (A-C) staining with uranyl acetate; (D) staining with phosphotungstic acid. HFTV1 particles devoid of DNA are indicated by arrows. Bars, 100 nm.

Figure 3. Lipid and protein analysis of virions. (A-C) A thin-layer chromatogram of lipids extracted from virus particles purified by PEG-NaCl precipitation, rate zonal (in sucrose) and equilibrium (in CsCl) centrifugation and concentrated by differential centrifugation (A) HRPV10, (B) HRPV11, and (C) HRPV12 and their corresponding host strains. The corresponding band of each lipid species are marked by 1-4. The major lipid species of *Haloarcula hispanica* (Hh) are indicated on the right and their positions marked by the Roman numerals as follows: PG, phosphatidylglycerol (I); PGP-Me, phosphatidylglycerophosphate methyl ester (II); PGS, phosphatidylglycerosulfate (III); TGD, triglycosyl glycerodiether (IV). (D-G) SDS-PAGE analysis of the purified viruses (D) HRPV10, (E) HRPV11, (F) HRPV12, (G) HFTV1. Molecular mass marker is shown (M, kDa).

Figure 4. Mung bean nuclease (MBN) analyses of (A) ϕX174 single-stranded (ss) and double-stranded (ds) genomic DNA (B) HRPV10, (C) HRPV11, and (D) HRPV12. MBN amounts used are indicated as units (U) per 1 µg of DNA. All reactions contained 300 ng of DNA. Molecular mass marker (M) is indicated in kb.

Figure 5. HRPV10, HRPV11, HRPV12 and the members of the family *Pleolipoviridae*. (A) Phylogenomic tree was constructed using the Genome BLAST Distance Phylogeny (GBDP) strategy implemented in VICTOR (Meier-Kolthoff and Goker, 2017). The numbers above branches are GBDP pseudo-bootstrap support values from 100 replications. Clades corresponding to the genera *Alphapleolipovirus*, *Betapleolipovirus* and *Gammapleolipovirus* are colored light blue, beige, and grey, respectively. (B) Genomic comparison of pleolipoviruses depicted in panel A. Homologous genes are indicated with the same colors.

Figure 6. Genomic comparison of HFTV1, HRTV-4, eHP-4, eHP-15 and eHP-1. Open reading frames (ORFs) are depicted as arrows indicating the directionality of transcription. When possible, the predicted functions are indicated above the corresponding ORFs. Shading connecting the ORFs indicates the amino acid sequence identity between the corresponding protein products; the color key is provided at the bottom of the figure. Abbreviations: TerS and TerL, small and large subunits of the terminase, respectively; CBD, carbohydrate-binding domain; PAPS, phosphoadenosine phosphosulfate; MCM, minichromosome maintenance helicase; PCNA, proliferating cell nuclear antigen; MTase, methyltransferase.

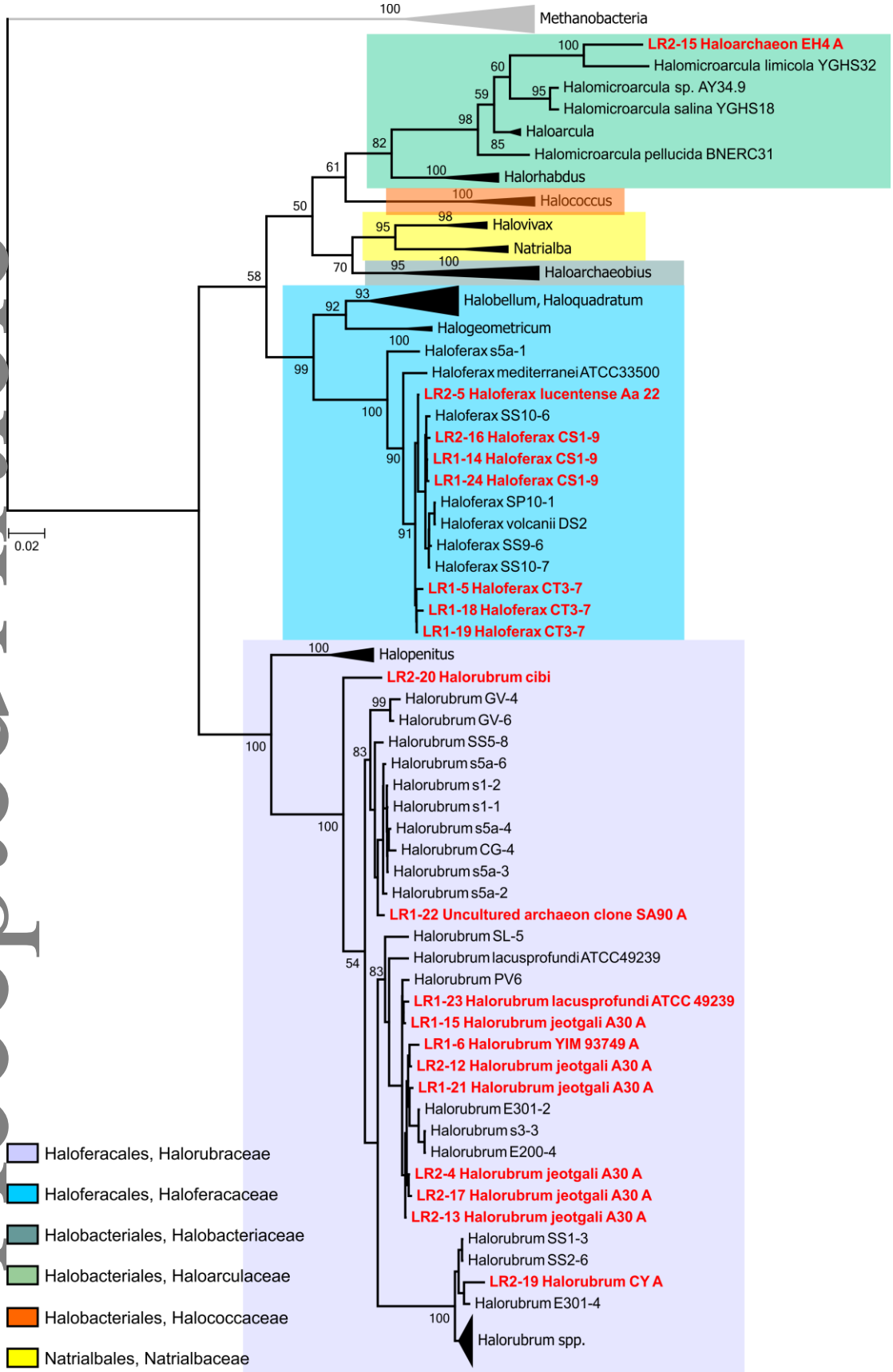

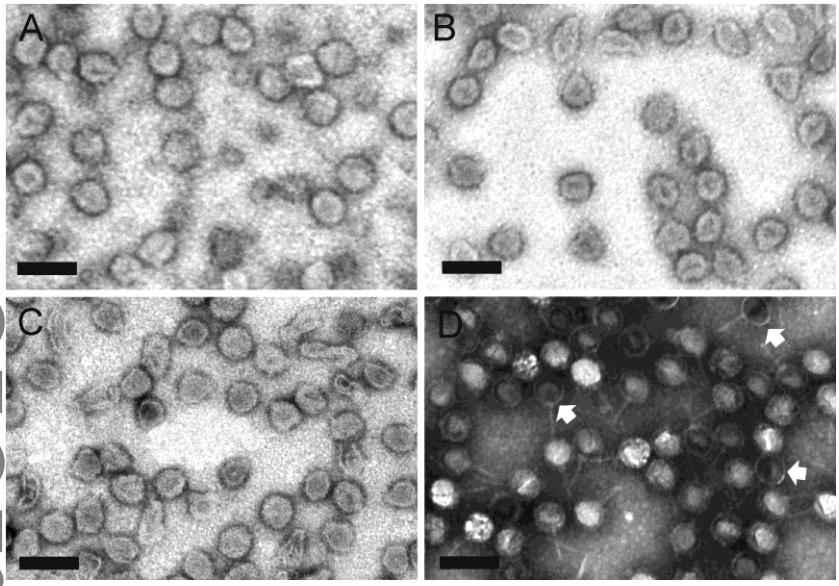

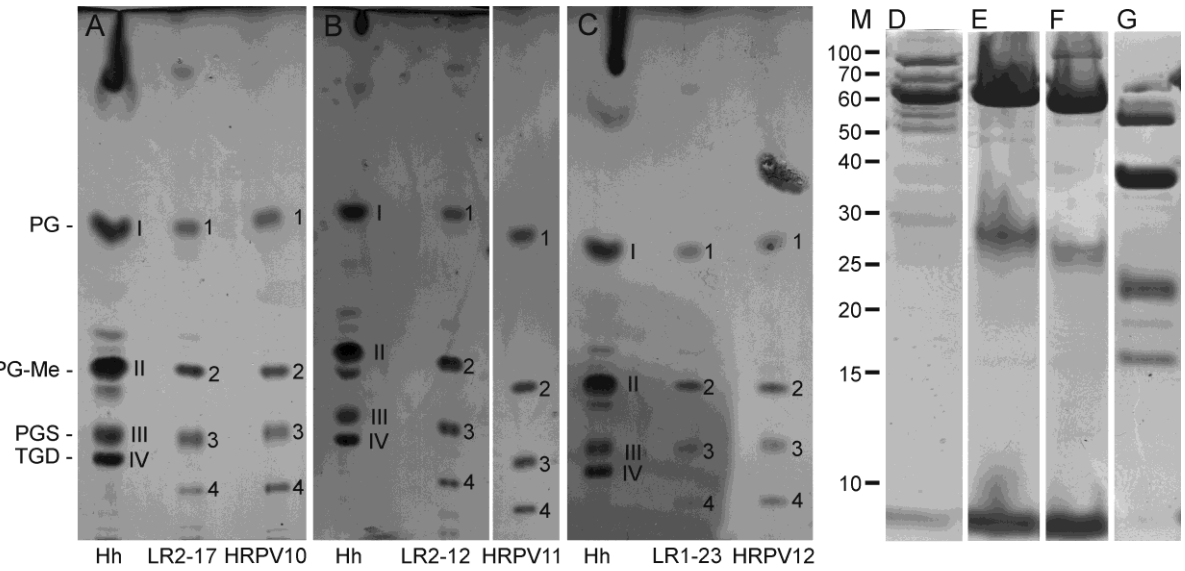

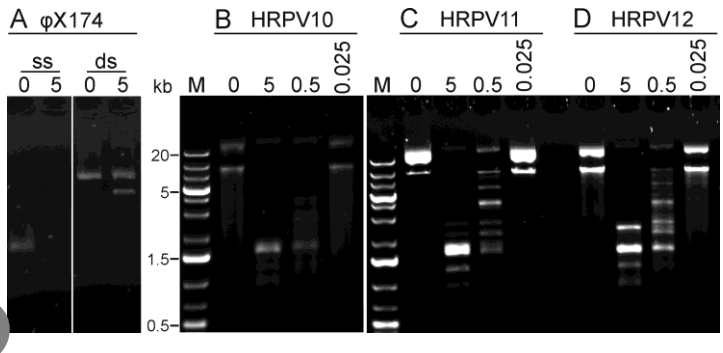

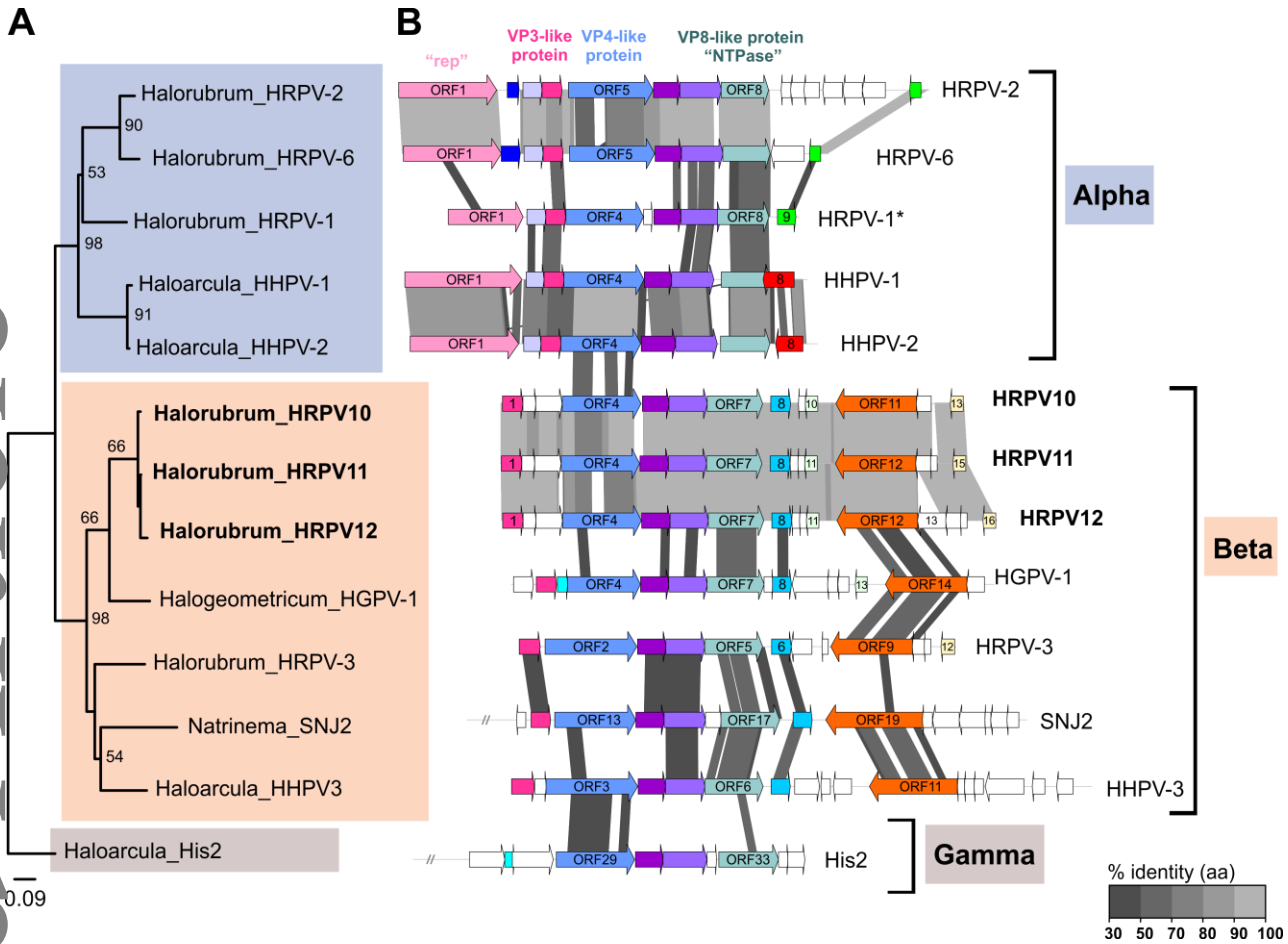

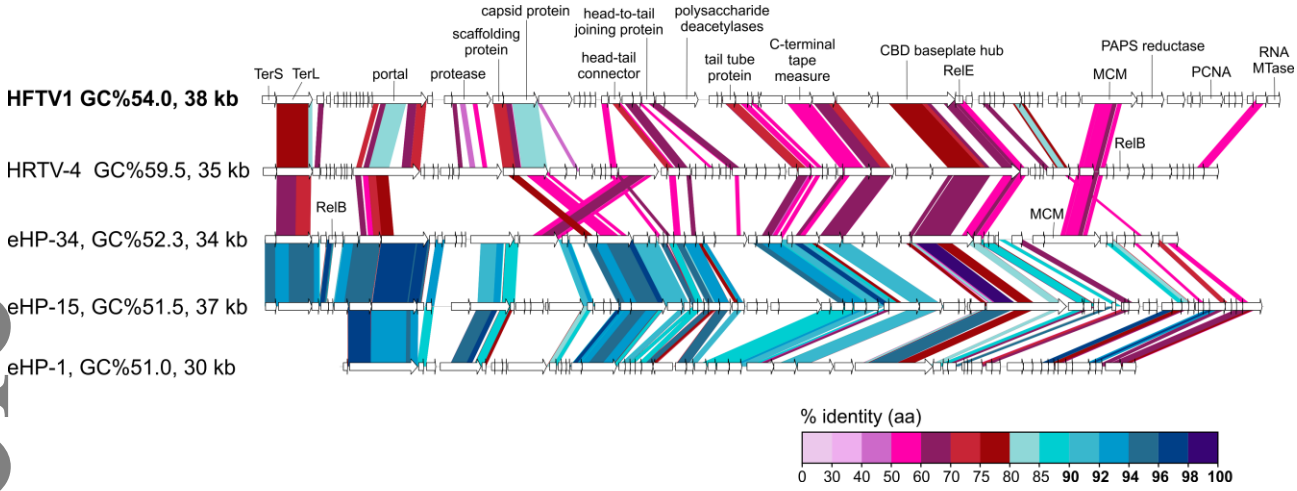

Table 1. Viruses from Lake Retba

Virus	Original host strain	Origin of the virus	Plaque morphology and diameter	Virus stock titer (pfu/ml)	Chloroform sensitivity[a]	Nonidet P-40 sensitivity[b]	Triton X-100 sensitivity[c]	Virion morphology
Halorubrum pleomorphic virus 10 (HRPV10)	*Halorubrum* sp. LR2-17	Sample LR2	Hazy, 3-5 mm	~1×10^{11}	Resistant	Sensitive, titer drops 11 logs	Sensitive, titer drops 11 logs	Pleomorphic
Halorubrum pleomorphic virus 11 (HRPV11)	*Halorubrum* sp. LR2-12	Sample LR2	Very hazy, 5-10 mm	~5×10^{11}	Sensitive, titer drops 2-3 logs	Sensitive, titer drops 8 logs	Sensitive, titer drops 11 logs	Pleomorphic
Halorubrum pleomorphic virus 12 (HRPV12)	*Halorubrum* sp. LR1-23	Sample LR1	Hazy, 5-8 mm	~1×10^{11}	Sensitive, titer drops ~1 log	Sensitive, titer drops 7 logs	Sensitive, titer drops 10 logs	Pleomorphic
Haloferax tailed virus 1 (HFTV1)	*Haloferax* sp. LR2-5	Sample LR2	Clear, 2-4 mm	~1×10^{12}	Resistant	Resistant	Resistant	Icosahedral, long non-contractile tail

[a] assayed by plaque assay in the presence of 20% (v/v) chloroform

[b] assayed by plaque assay in the presence of 0.1 % (v/v) Nonidet P-40

[c] assayed by plaque assay in the presence of 0.1 % (v/v) Triton-X-100

Table 2. Strains isolated from the Lake Retba samples

Strains	Origin[a]	16S rRNA sequence Acc. No; length (bp)	Efficiency of plating[b]			
			HRPV10	HRPV11	HRPV12	HFTV1
Haloferax sp. LR1-5	LR1	MG462733; 1443				
Haloferax sp. LR1-14	LR1	MG462735; 1529				
Haloferax sp. LR1-18	LR1	MG462745; 1443				
Haloferax sp. LR1-19	LR1	MG462736; 1443				
Haloferax sp. LR1-24	LR1	MG462739; 1443				
Haloferax sp. LR2-5	LR2	MG462740; 1443				1 (H)
Haloferax sp. LR2-16	LR2	MG462742; 1443				
Halomicroarcula sp. LR2-15	LR2	MG462749; 1442				
Halorubrum sp. LR1-6	LR1	MG462734; 1440				
Halorubrum sp. LR1-15	LR1	MG462744; 1440		$\sim 7\times10^{-4}$		
Halorubrum sp. LR1-21	LR1	MG462746; 1440		$\sim 2\times10^{-1}$		
Halorubrum sp. LR1-22	LR1	MG462737; 1440				
Halorubrum sp. LR1-23	LR1	MG462738; 1440			1 (H)	$\sim 5\times10^{-8}$
Halorubrum sp. LR2-4	LR2	MG462747; 1436				
Halorubrum sp. LR2-12	LR2	MG462741; 1441	$\sim 1\times10^{-3}$	1 (H)	$\sim 2\times10^{-4}$	
Halorubrum sp. LR2-13	LR2	MG462748; 1440		$\sim 9\times10^{-3}$		
Halorubrum sp. LR2-17	LR2	MG462750; 1440	1 (H)			
Halorubrum sp. LR2-19	LR2	MG462751; 1440				
Halorubrum sp. LR2-20	LR2	MG462743; 1441				

a. LR1, Lake Retba sample 1; LR2, Lake Retba sample 2

b. The sensitivities of the archaeal strains to isolated viruses (Table 1) are shown as efficiency of plating (EOP) measured as plaque forming units. For the original host (marked by H), the EOP was set to a value of 1. EOPs on others strains are relative to the EOP of the original host.

Table 3. Virus purification by PEG-NaCl precipitation, rate zonal (in sucrose), equilibrium (in CsCl) and differential ultracentrifugation

Virus	Number of the infections purified viruses (total pfus)[a]	Recovery of the infectious purified viruses[b] (%)	Yield of the purified viruses in protein (total mg of protein)[c]	Specific infectivity of the purified viruses (pfu / mg of protein)
HRPV10	~2×10^{13}	~11	~0.8	~3×10^{13}
HRPV11	~7×10^{13}	~15	~1.5	~5×10^{13}
HRPV12	~8×10^{12}	~8	~0.4	~2×10^{13}
HFTV1	~3×10^{9}	~0.0005	~1.9	~2×10^{9}

[a] Total pfus (purified viruses) obtained from a liter of virus stock

[b] Calculated based on the total pfus in the starting material (virus stocks; see the virus stock titers in Table 1) and the final sample (purified viruses)

[c] Total mg of protein (purified viruses) obtained from a liter of virus stock